Precision QCD in DIS at HERA

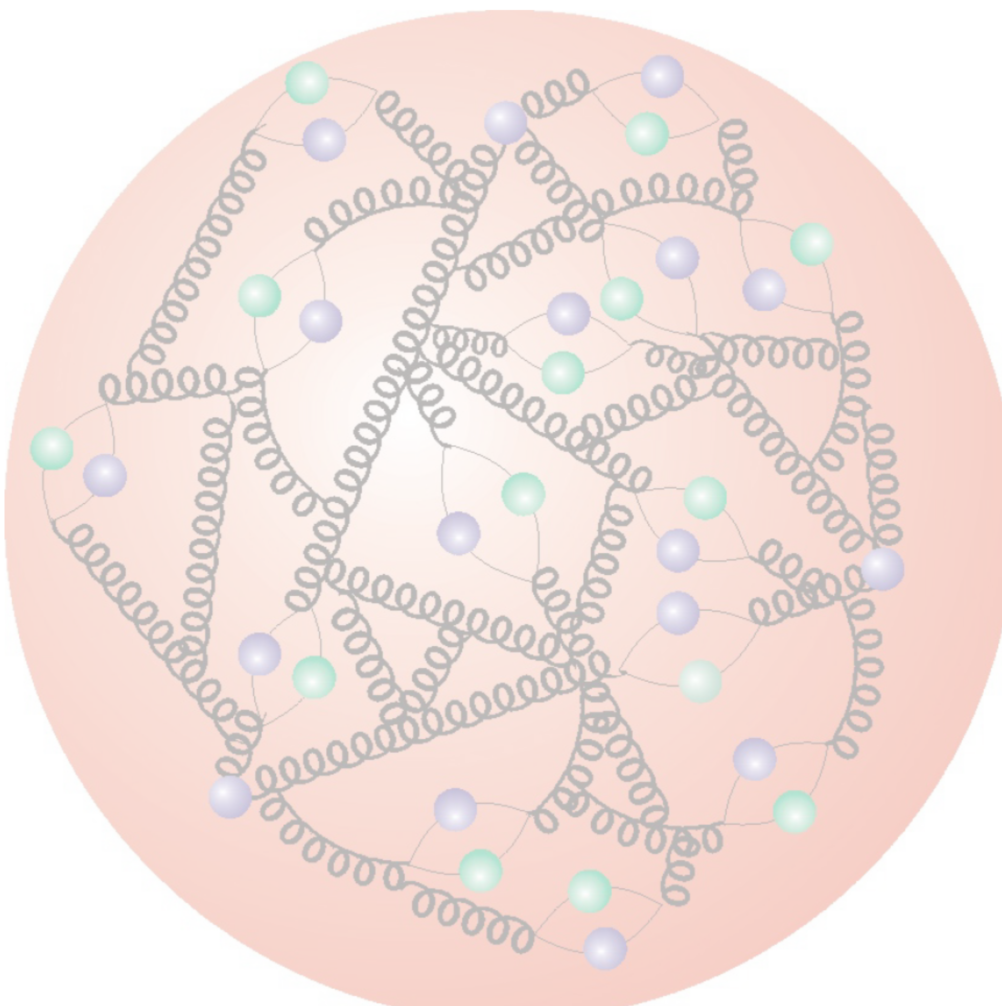

- Introduction
- HERA-II Updates
- H1 NC/CC $e^{\pm}p$
- H1 NC High y $e^{\pm}p$
- ZEUS NC $e^{+}p$
- HERAPDF Plans

Queen Mary University of London

Eram Rizvi

PDF4LHC

CERN – 7th Oct. 2012

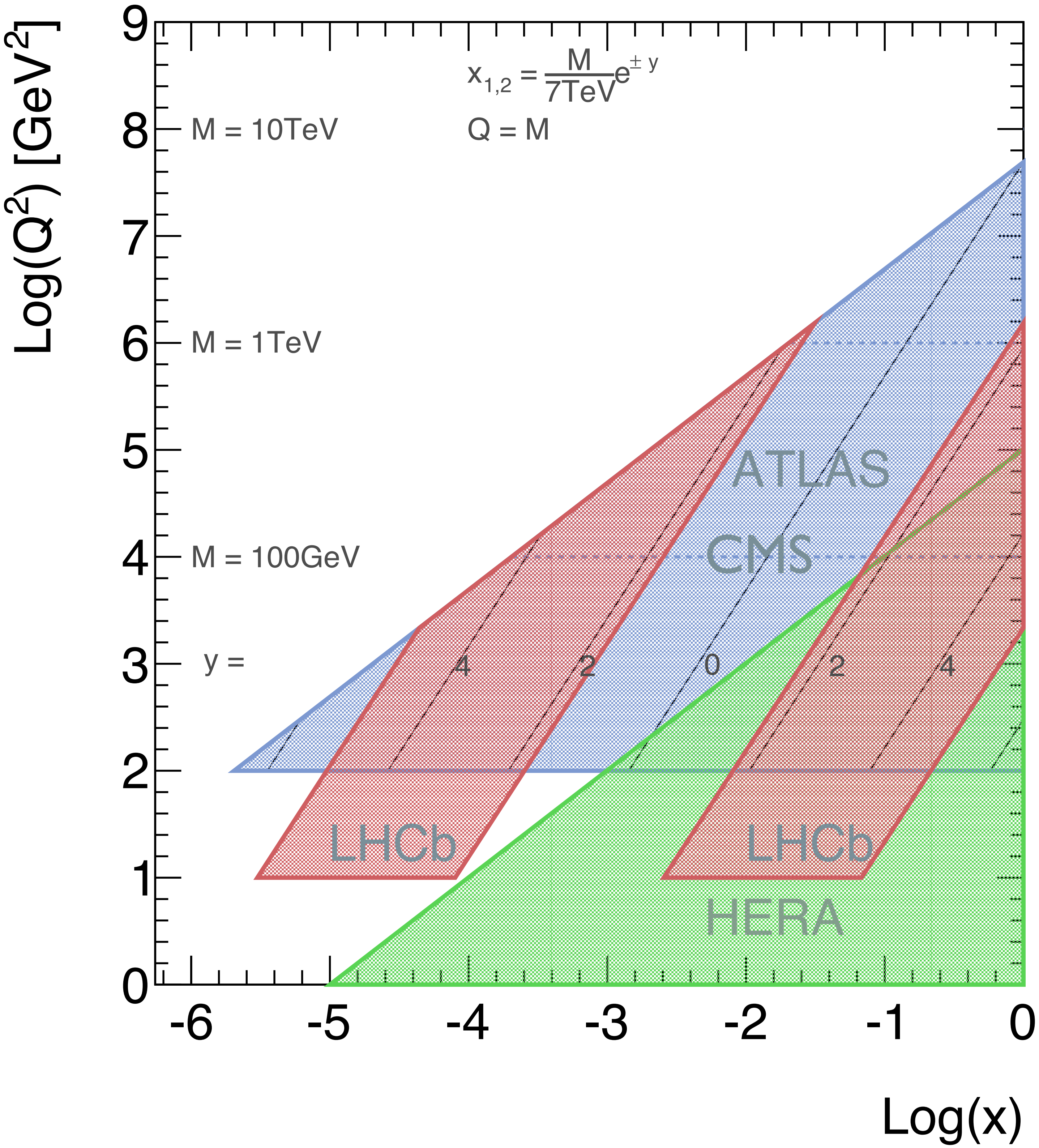

LHC: largest mass states at large x

For central production $x=x_1=x_2$

$M=x\sqrt{s}$

i.e. M > 1 TeV probes x>0.1

Searches for high mass states require precision knowledge at high x

Z′ / quantum gravity / susy searches...

DGLAP evolution allows predictions to be made

High x predictions rely on

- data (DIS / fixed target)
- sum rules
- behaviour of PDFs as $x \to 1$

$$\frac{d\sigma^{\pm}_{NC}}{dxdQ^2} = \frac{2\pi\alpha^2}{x} \left[\frac{1}{Q^2}\right]^2 \left[Y_+\tilde{F}_2 \mp Y_- x\tilde{F}_3 - y^2\tilde{F}_L\right]$$

$$\frac{d\sigma^{\pm}_{CC}}{dxdQ^2} = \frac{G_F^2}{4\,\pi\,x} \left[\frac{M_W^2}{M_W^2+Q^2}\right]^2 \left[Y_+\,\tilde{W}_2^{\pm} \mp Y_-\,x\tilde{W}_3^{\pm} - y^2\tilde{W}_L^{\pm}\right]$$

$$Y_{\pm} = 1 \pm (1-y)^2$$

$$\tilde{F}_2 \propto \sum (xq_i + x\bar{q}_i)$$

Dominant contribution

$$x\tilde{F}_3 \propto \sum (xq_i - x\bar{q}_i)$$

Only sensitive at high $Q^2 \sim M_Z^2$

$$\tilde{F}_L \propto \alpha_s \cdot xg(x,Q^2)$$

Only sensitive at low Q^2 and high y

similarly for pure weak CC analogues:

$W_2^{\pm}$, $xW_3^{\pm}$ and $W_L^{\pm}$

The NC reduced cross section defined as:

$$\tilde{\sigma}^{\pm}_{NC} = \frac{Q^2 x}{2\alpha\pi^2}\frac{1}{Y_+}\frac{d^2\sigma^{\pm}}{dxdQ^2}$$

$$\tilde{\sigma}^{\pm}_{NC} \sim \tilde{F}_2 \mp \frac{Y_-}{Y_+} x\tilde{F}_3$$

The CC reduced cross section defined as:

$$\sigma^{\pm}_{CC} = \frac{2\pi x}{G_F^2}\left[\frac{M_W^2+Q^2}{M_W^2}\right]^2 \frac{d\sigma^{\pm}_{CC}}{dxdQ^2}$$

$$\frac{d\sigma^{\pm}_{CC}}{dxdQ^2} = \frac{1}{2}\left[Y_+\,W_2^{\pm} \mp Y_-\,xW_3^{\pm} - y^2 W_L^{\pm}\right]$$

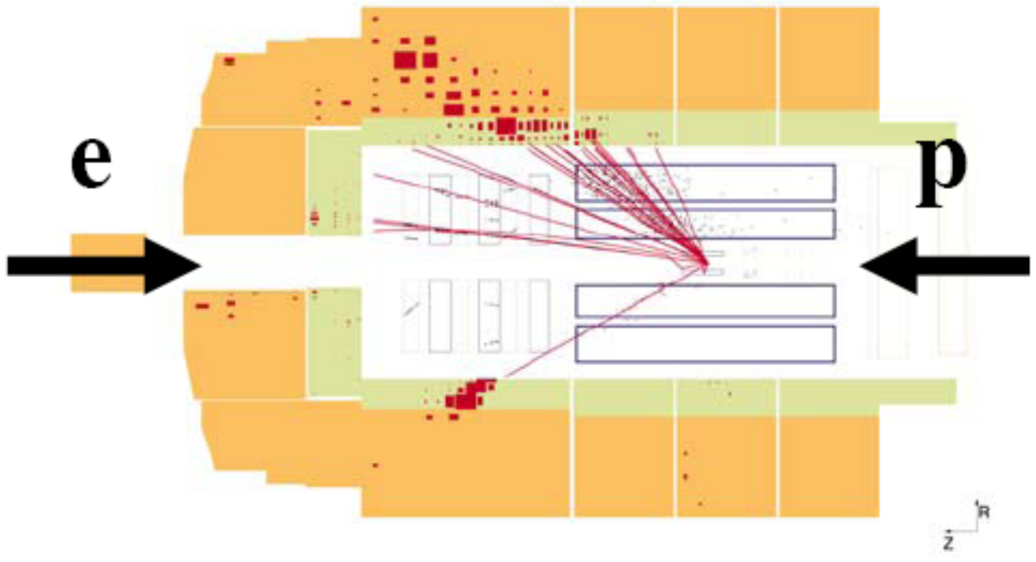

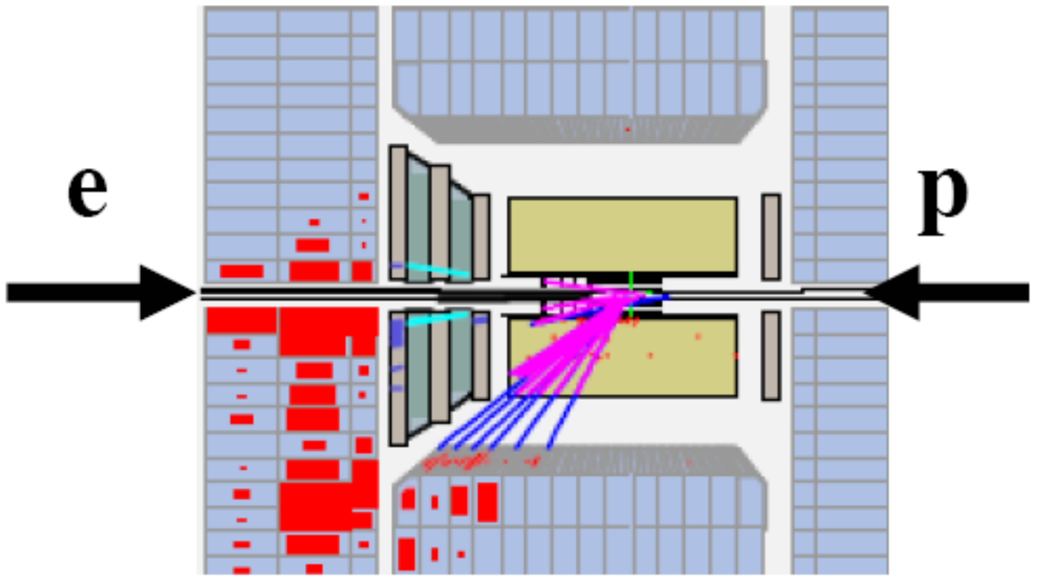

Neutral current event selection:

High P_T isolated scattered lepton
Suppress huge photo-production background by imposing longitudinal energy-momentum conservation

Kinematics may be reconstructed in many ways:
energy/angle of hadrons & scattered lepton
provides excellent tools for sys cross checks

Removal of scattered lepton provides a
high stats "pseudo-charged current sample"
Excellent tool to cross check CC analysis

Final selection: $\sim 10^5$ events per sample at high Q^2
$\sim 10^7$ events for $10 < Q^2 < 100$ GeV^2

Charged current event selection:

Large missing transverse momentum (neutrino)

Suppress huge photo-production background

Topological finders to remove cosmic muons

Kinematics reconstructed from hadrons

Final selection: $\sim 10^3$ events per sample

HERA Operation

HERA-I operation 1993-2000
Ee = 27.6 GeV
Ep = 820 / 920 GeV
$\int\mathcal{L}$ ~ 110 pb^{-1} per experiment

HERA-II operation 2003-2007
Ee = 27.6 GeV
Ep = 920 GeV
$\int\mathcal{L}$ ~ 330 pb^{-1} per experiment
Longitudinally polarised leptons

Low Energy Run 2007
Ee = 27.6 GeV
Ep = 575 & 460 GeV
Dedicated F_L measurement

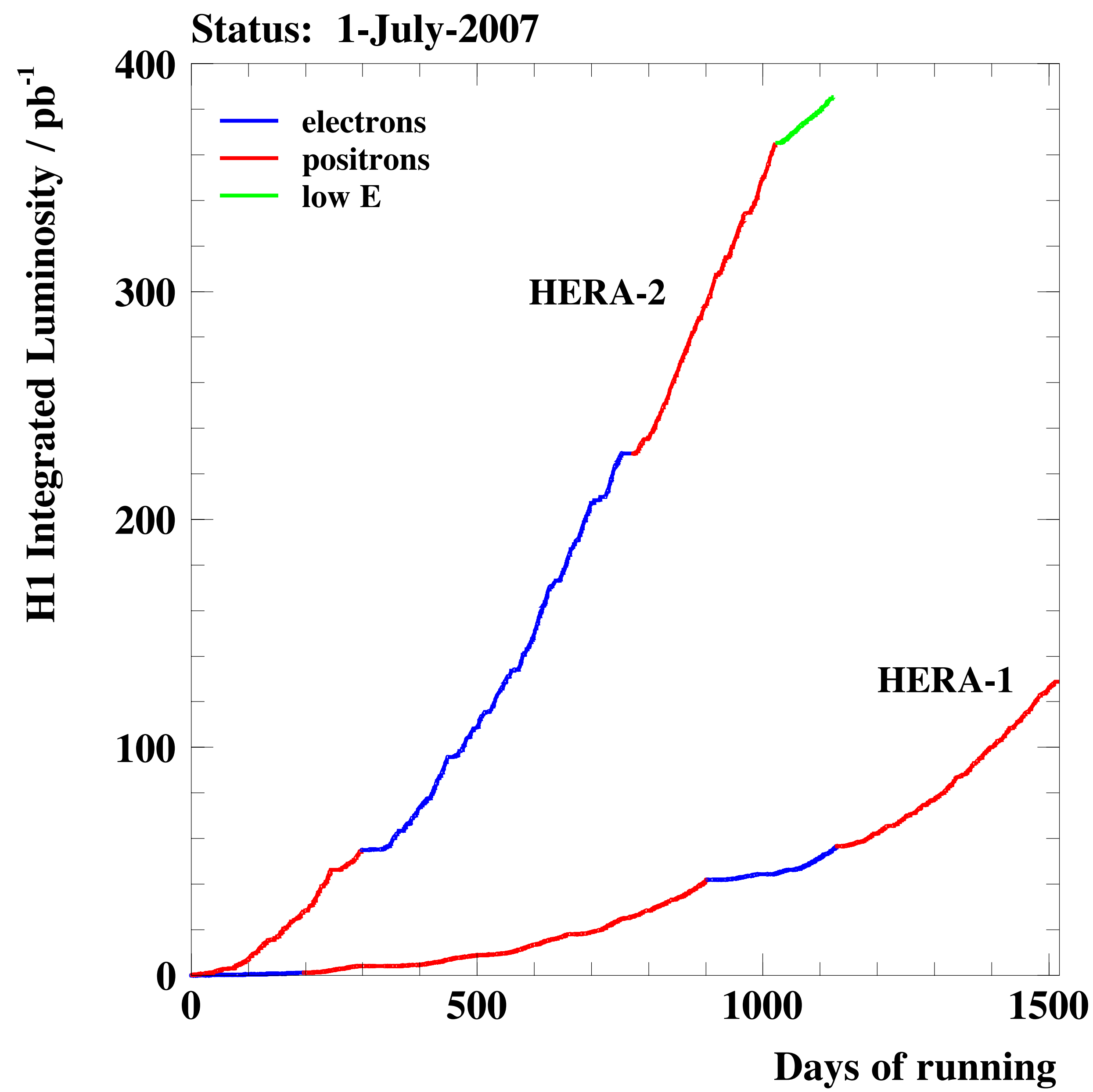

breakdown of HERA-II data samples

	R	L
e^-p	$\mathcal{L} = 47.3\,\text{pb}^{-1}$ $P_e = (+36.0 \pm 1.0)\%$	$\mathcal{L} = 104.4\,\text{pb}^{-1}$ $P_e = (-25.8 \pm 0.7)\%$
e^+p	$\mathcal{L} = 101.3\,\text{pb}^{-1}$ $P_e = (+32.5 \pm 0.7)\%$	$\mathcal{L} = 80.7\,\text{pb}^{-1}$ $P_e = (-37.0 \pm 0.7)\%$

HERA Structure Function Data

Summary of HERA-I datasets
Combined in HERAPDF1.0

Available since 2009

Data Set		x Range		Q^2 Range GeV^2		$\mathcal{L}$ pb^{-1}	e^+/e^-	$\sqrt{s}$ GeV
H1 svx-mb	95-00	5×10^{-6}	0.02	0.2	12	2.1	e^+p	301-319
H1 low Q^2	96-00	2×10^{-4}	0.1	12	150	22	e^+p	301-319
H1 NC	94-97	0.0032	0.65	150	30000	35.6	e^+p	301
H1 CC	94-97	0.013	0.40	300	15000	35.6	e^+p	301
H1 NC	98-99	0.0032	0.65	150	30000	16.4	e^-p	319
H1 CC	98-99	0.013	0.40	300	15000	16.4	e^-p	319
H1 NC HY	98-99	0.0013	0.01	100	800	16.4	e^-p	319
H1 NC	99-00	0.0013	0.65	100	30000	65.2	e^+p	319
H1 CC	99-00	0.013	0.40	300	15000	65.2	e^+p	319
ZEUS BPC	95	2×10^{-6}	6×10^{-5}	0.11	0.65	1.65	e^+p	301
ZEUS BPT	97	6×10^{-7}	0.001	0.045	0.65	3.9	e^+p	301
ZEUS SVX	95	1.2×10^{-5}	0.0019	0.6	17	0.2	e^+p	301
ZEUS NC	96-97	6×10^{-5}	0.65	2.7	30000	30.0	e^+p	301
ZEUS CC	94-97	0.015	0.42	280	17000	47.7	e^+p	301
ZEUS NC	98-99	0.005	0.65	200	30000	15.9	e^-p	319
ZEUS CC	98-99	0.015	0.42	280	30000	16.4	e^-p	319
ZEUS NC	99-00	0.005	0.65	200	30000	63.2	e^+p	319
ZEUS CC	99-00	0.008	0.42	280	17000	60.9	e^+p	319

High Q^2 NC and CC data limited to
100 pb^{-1} e^+p
16 pb^{-1} e^-p

HERA Structure Function Data

Up till now HERA-II datasets only partially published

ZEUS CC e^-p	175 pb^{-1}	EPJ C 61 (2009) 223-235
ZEUS CC e^+p	132 pb^{-1}	EPJ C 70 (2010) 945-963
ZEUS NC e^-p	170 pb^{-1}	EPJ C 62 (2009) 625-658
ZEUS NC e^+p	135 pb^{-1}	ZEUS-prel-11-003
H1 CC e^-p	149 pb^{-1}	H1prelim-09-043
H1 CC e^+p	180 pb^{-1}	H1prelim-09-043
H1 NC e^-p	149 pb^{-1}	H1prelim-09-042
H1 NC e^+p	180 pb^{-1}	H1prelim-09-042

HERA-II datasets
Combined in HERAPDF1.5
(except ZEUS NC e^+p)

↓

ZEUS CC e^-p	175 pb^{-1}	EPJ C 61 (2009) 223-235
ZEUS CC e^+p	132 pb^{-1}	EPJ C 70 (2010) 945-963
ZEUS NC e^-p	170 pb^{-1}	EPJ C 62 (2009) 625-658
ZEUS NC e^+p	135 pb^{-1}	**arXiv:1208.6138**
H1 CC e^-p	149 pb^{-1}	**arXiv:1206.7007**
H1 CC e^+p	180 pb^{-1}	
H1 NC e^-p	149 pb^{-1}	
H1 NC e^+p	180 pb^{-1}	

Complete the analyses of HERA high Q^2 inclusive structure function data

New published data increase $\int\mathcal{L}$ by
~ factor 3 for e^+p
~ factor 10 for e^-p
much improved systematic uncertainties

High Q^2 NC Cross Sections

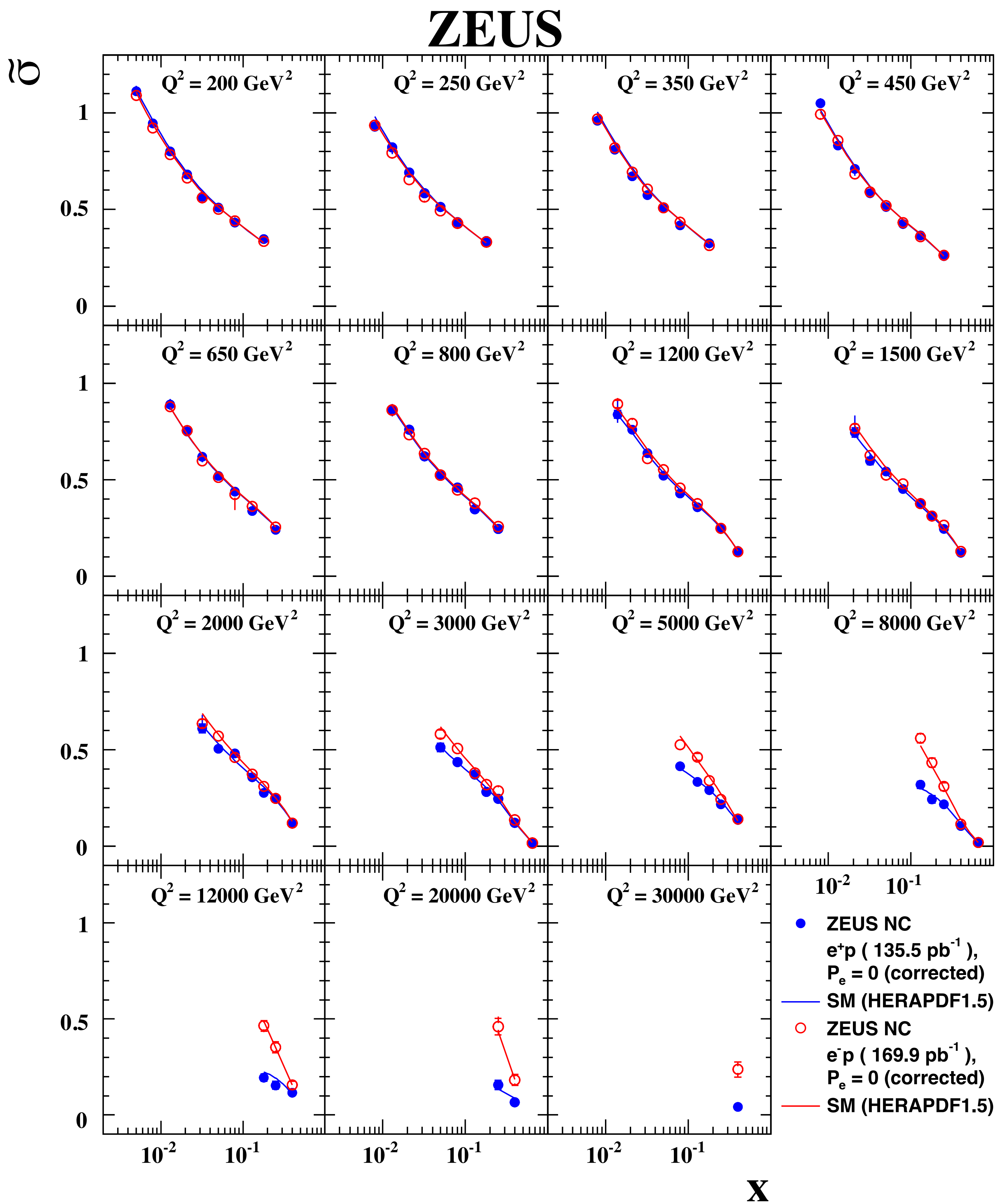

High Q^2 is the EW physics regime:
Z^0 contribution enhances as Q^2 increases

Final measurement of ZEUS NC e^+p data

Shown here for P=0
Polarised measurements also available

Compared to published NC e^-p data

High Q^2 NC Cross Sections

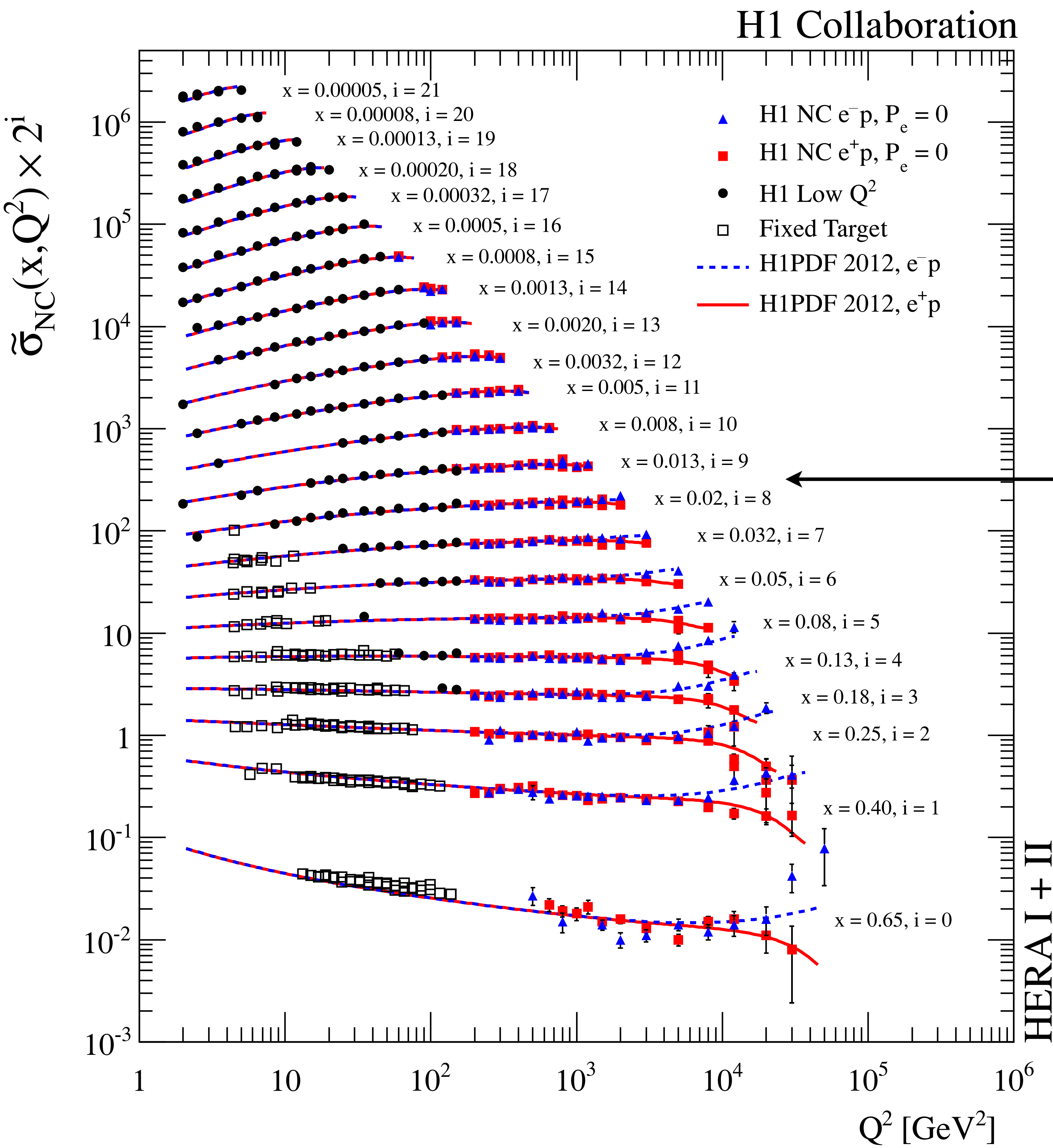

H1 precision 1.5% for $Q^2 < 500$ GeV^2
⇒ factor 2 reduction in error wrt HERA-I

Statistics limited at higher Q^2 and high x

Extended reach at high x compared to H1 preliminary data

This x region is the 'sweet spot'
High precision with long Q^2 lever arm
x-range relevant for Higgs production

Combination of high Q^2 data
HERA-I and HERA-II

Larger HERA-II luminosity
→ improved precision at high x / Q^2

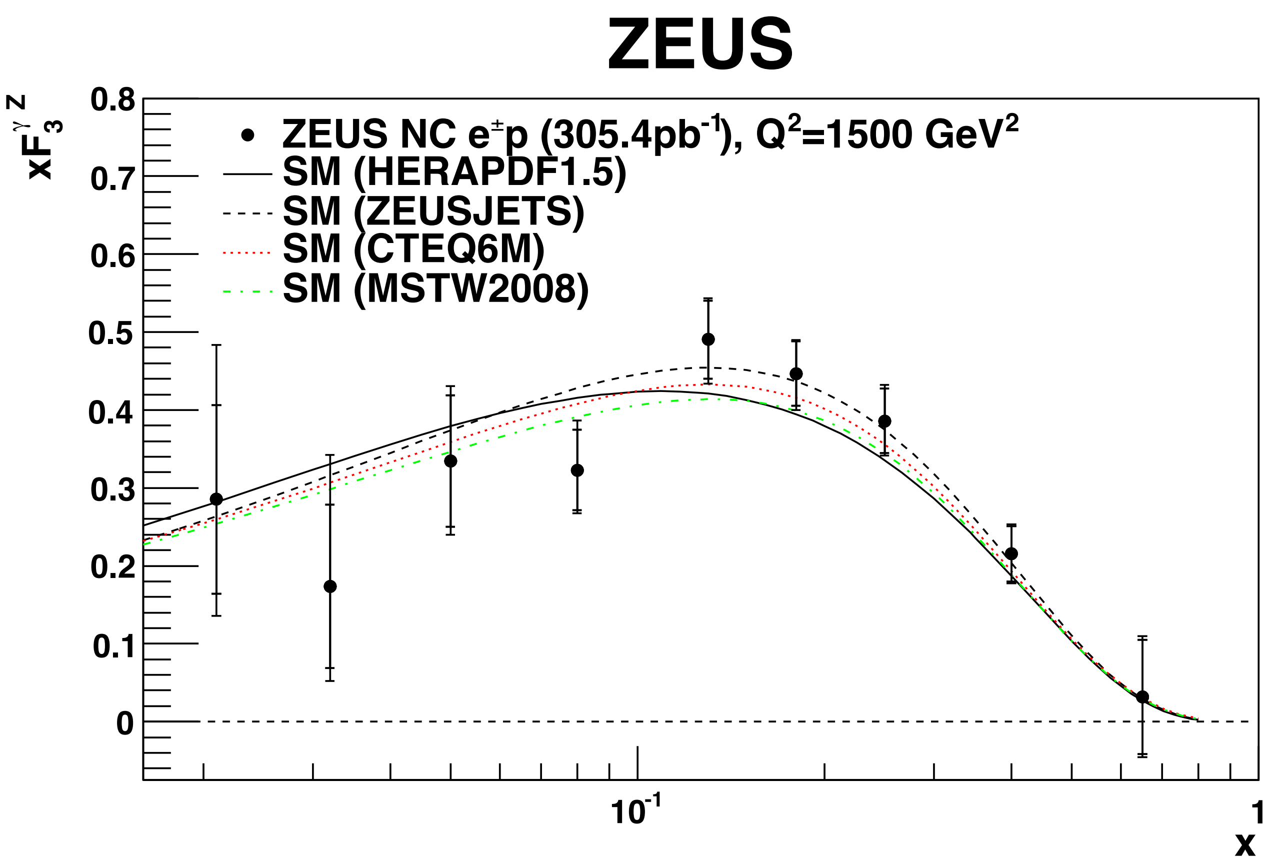

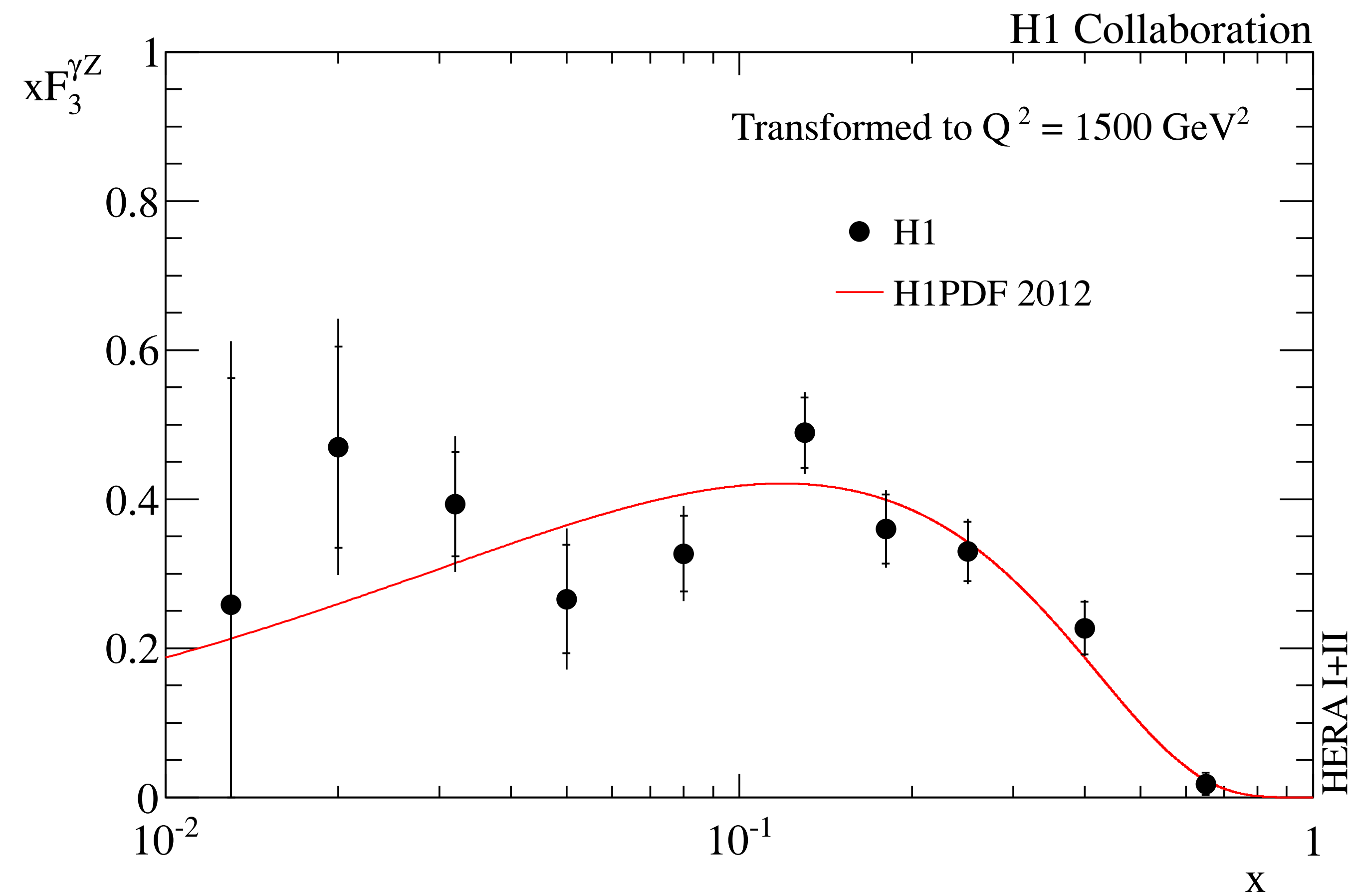

At high Q² xF3 arises due to Z⁰ effects
enhanced e⁻ cross section wrt e⁺
Difference is xF3
Sensitive to valence PDFs

$$x\tilde{F}_3 = \frac{Y_+}{2Y_-}(\tilde{\sigma}^-_{NC} - \tilde{\sigma}^+_{NC}) \quad \approx \quad a_e \chi_Z x F_3^{\gamma Z}$$

$$x\tilde{F}_3 \propto \sum (xq_i - x\bar{q}_i)$$

H1 measure integral of $xF_3^{\gamma Z}$ - validate sumrule:

$$\int_{0.016}^{0.725} \mathrm{d}x \; F_3^{\gamma Z}(x, Q^2 = 1\,500\,\mathrm{GeV}^2) = 1.22 \pm 0.09(\mathrm{stat}) \pm 0.07(\mathrm{syst})$$

NLO integral predicted to be $5/3 + \mathcal{O}(\alpha_S/\pi) = 1.16$

NC Cross Sections at High y

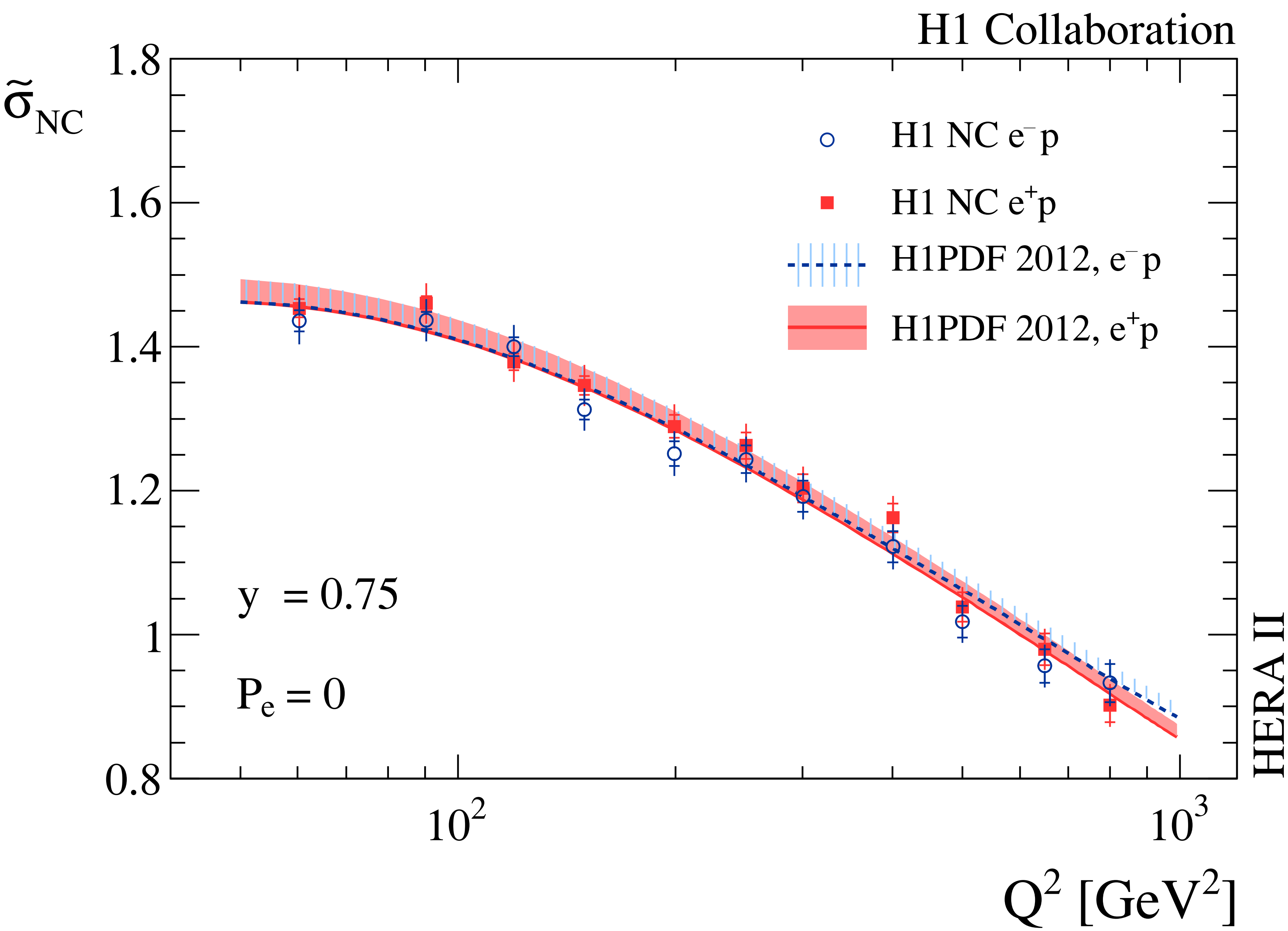

Measurement extension to high y at high Q^2

Sensitive to F_L and xg

Difficult measurement:
- low scattered electron energy $E_e' > 5$ GeV
- large photoproduction background

Total uncertainty reduced by factor 2:
HERA-I ~4%
HERA-II ~2%

High Q^2 CC Cross Sections

Electron scattering

$$\frac{d^2\sigma^-_{CC}}{dxdQ^2} = \frac{G_F^2}{2\pi}\left(\frac{M_W^2}{M_W^2+Q^2}\right)^2\left[(u+c)+(1-y)^2(\bar{d}+\bar{s})\right]$$

Positron scattering

$$\frac{d^2\sigma^+_{CC}}{dxdQ^2} = \frac{G_F^2}{2\pi}\left(\frac{M_W^2}{M_W^2+Q^2}\right)^2\left[(\bar{u}+\bar{c})+(1-y)^2(d+s)\right]$$

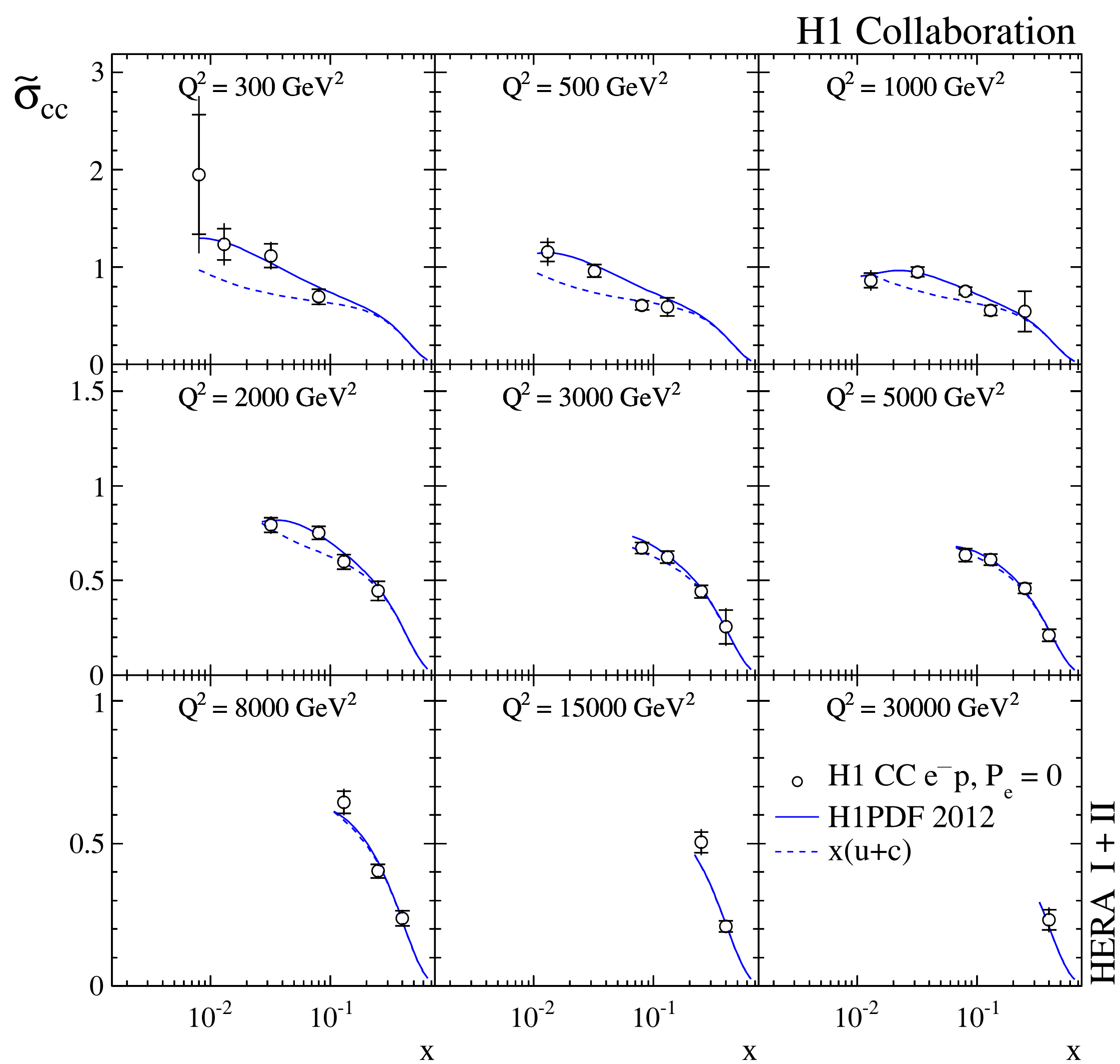

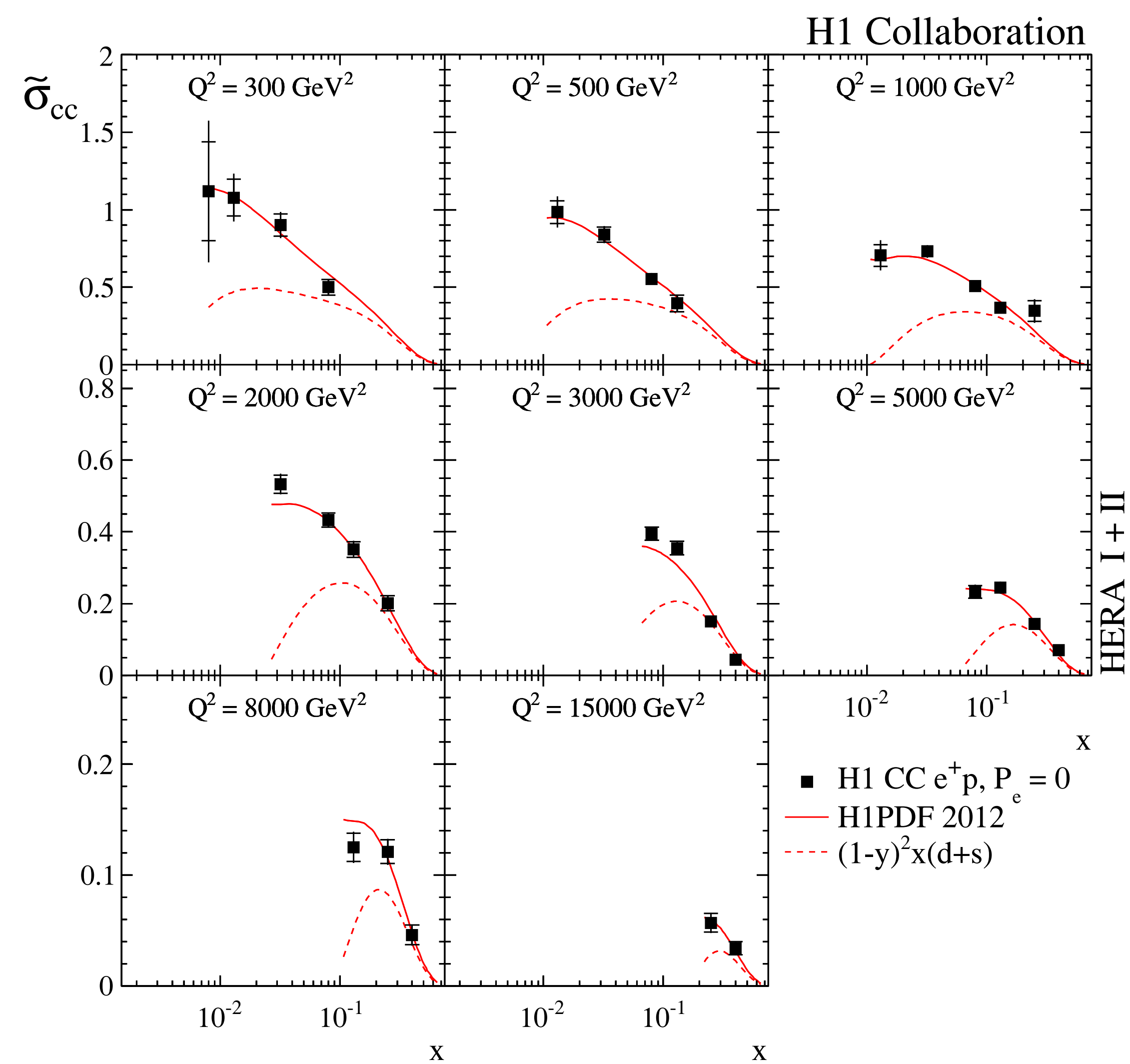

H1 combination of high Q^2 CC data (HERA-I+II)
Improvement of total uncertainty
Dominated by statistical errors
Provide important flavour decomposition information

CC e+ data provide strong d_v constraint at high x
Precision limited by statistics: typically 5-10%
HERA-I precision of 10-15% for e+p
Large gain to come after combination with ZEUS

CC Polarisation Dependence

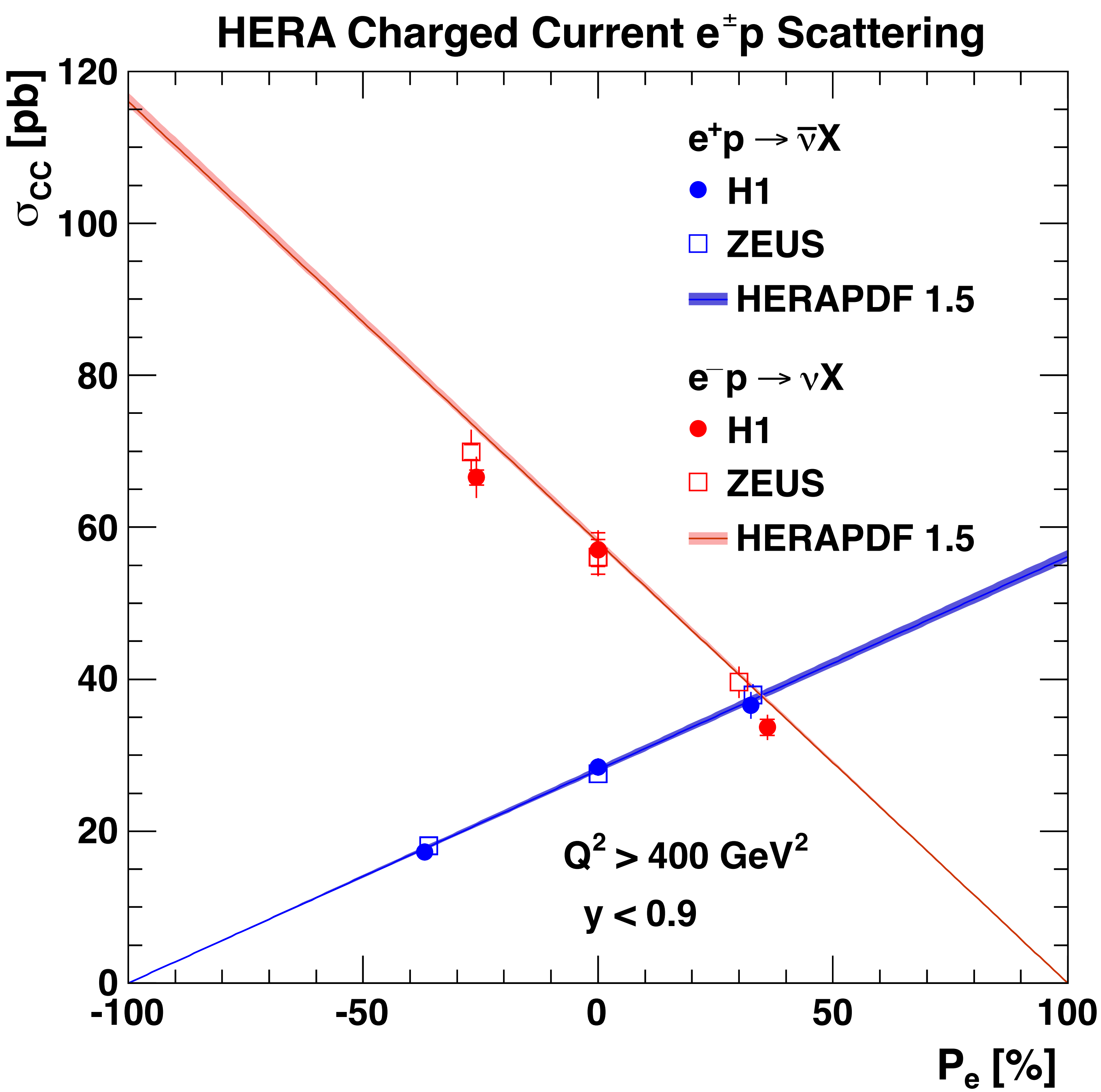

Polarisation dependence of CC cross section now final from H1 and ZEUS

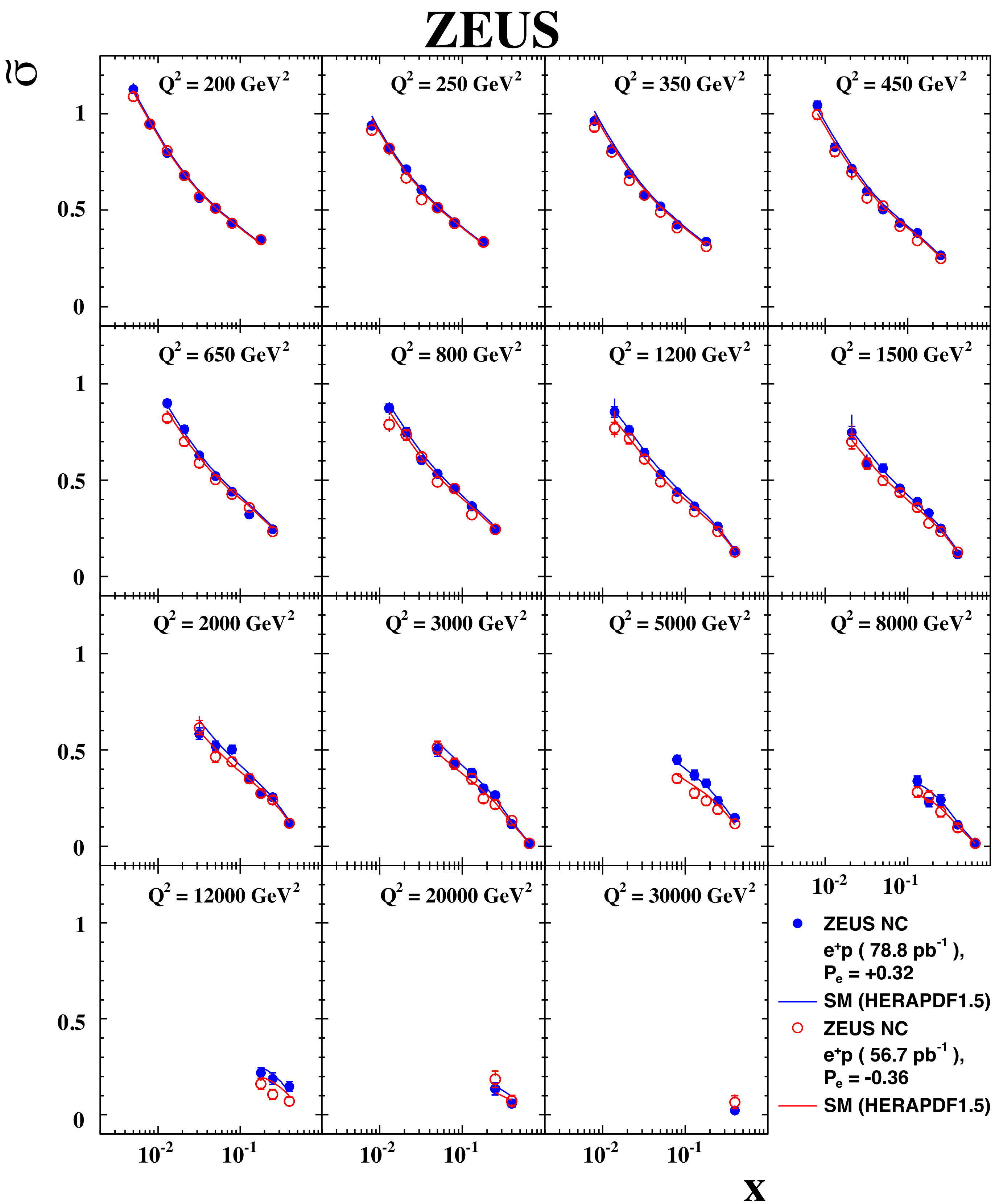

Polarised NC measurements completed for e^+p , e^-p , L-handed , R-handed scattering

Difference in L,R scattering visible at high Q^2

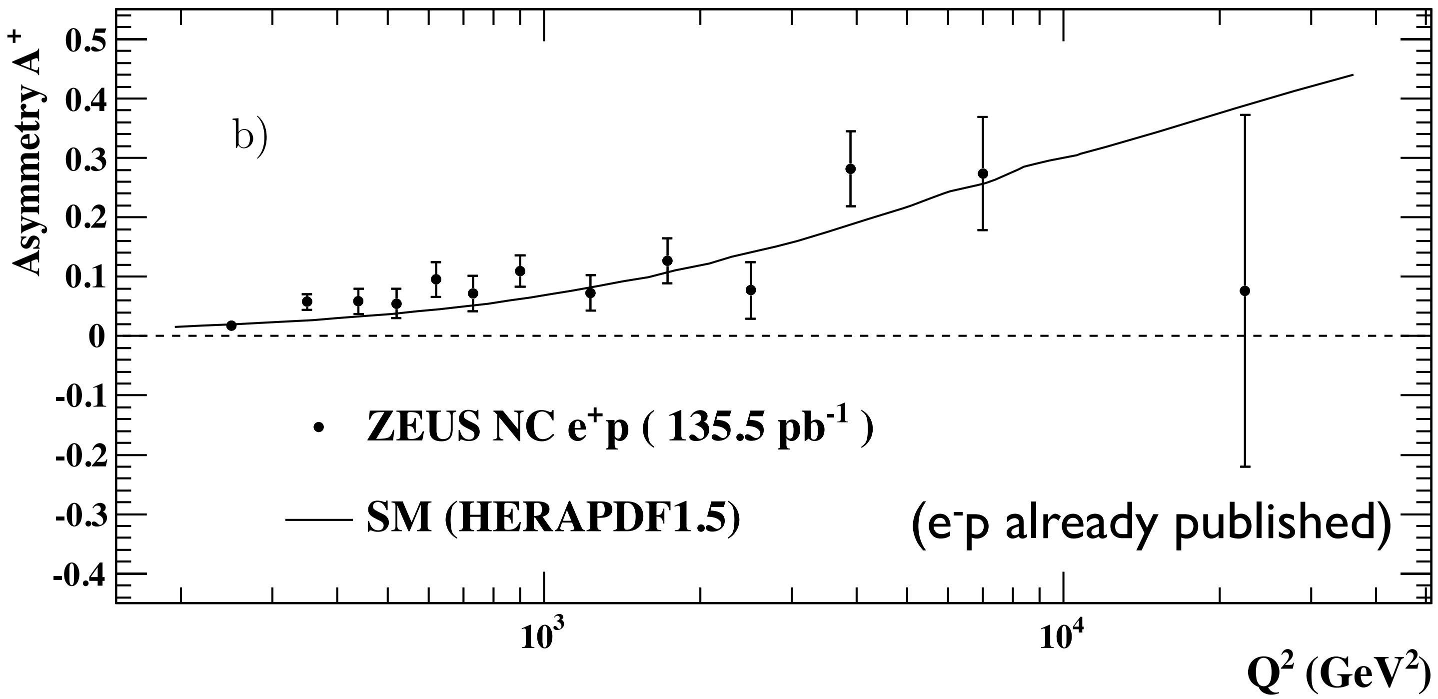

NC polarisation asymmetry:

$$A^{\pm} = \frac{2}{P_L^{\pm} - P_R^{\pm}} \cdot \frac{\sigma^{\pm}(P_L^{\pm}) - \sigma^{\pm}(P_R^{\pm})}{\sigma^{\pm}(P_L^{\pm}) + \sigma^{\pm}(P_R^{\pm})}$$

At large x $A^{\pm} \propto \pm\kappa \frac{1 + d_v/u_v}{4 + d_v/u_v}$

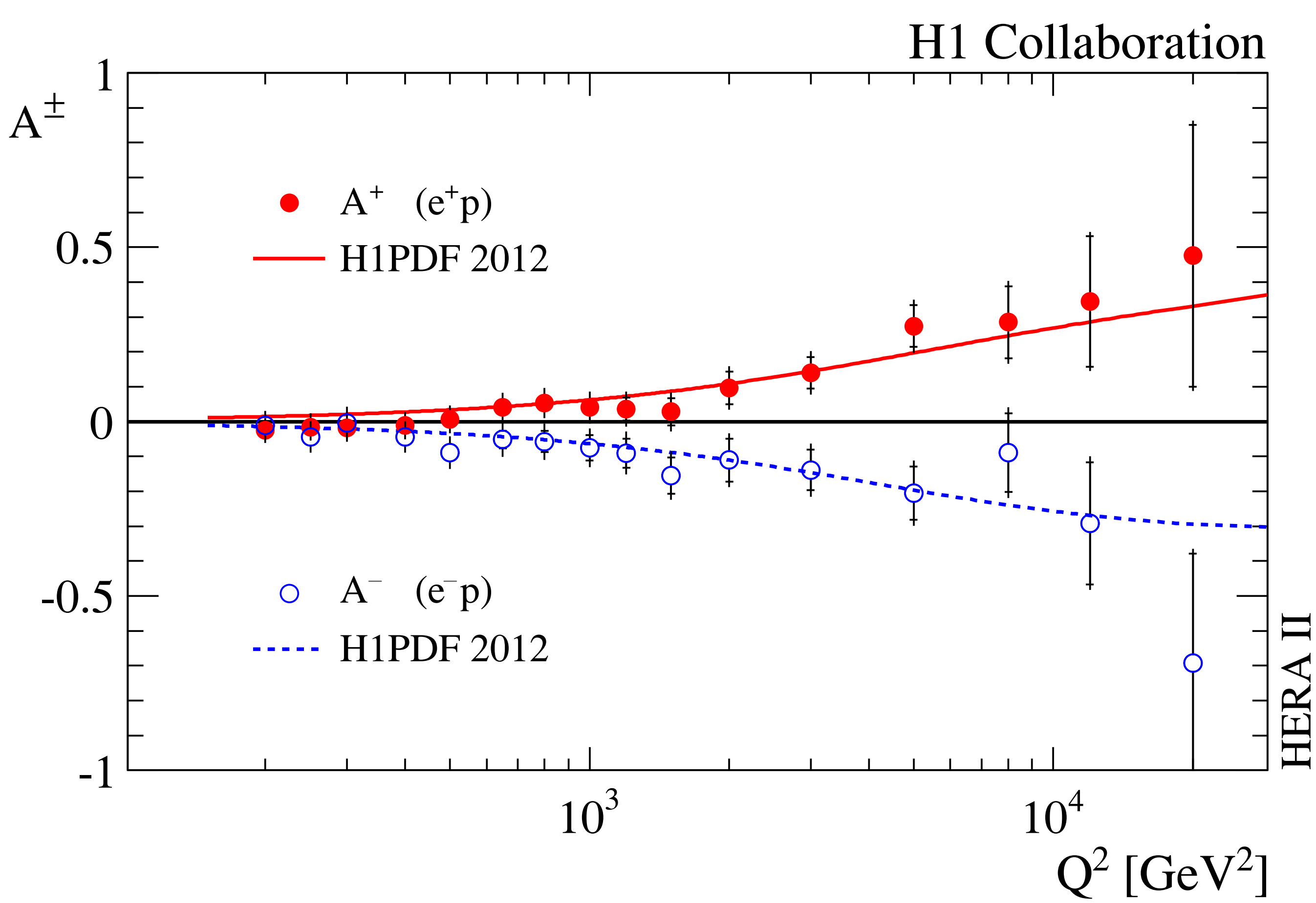

Measuring the difference in NC polarised cross sections gives access to new structure functions:

$$\frac{\sigma^{\pm}(P_L^{\pm}) - \sigma^{\pm}(P_R^{\pm})}{P_L^{\pm} - P_R^{\pm}} = \frac{\kappa Q^2}{Q^2 + M_Z^2}\left[\mp a_e F_2^{\gamma Z} + \frac{Y_-}{Y_+} v_e x F_3^{\gamma Z} - \frac{Y_-}{Y_+}\frac{\kappa Q^2}{Q^2 + M_Z^2}(v_e^2 + a_e^2) x F_3^Z\right]$$

xF_3 terms eliminated by subtracted e^-p from e^+p

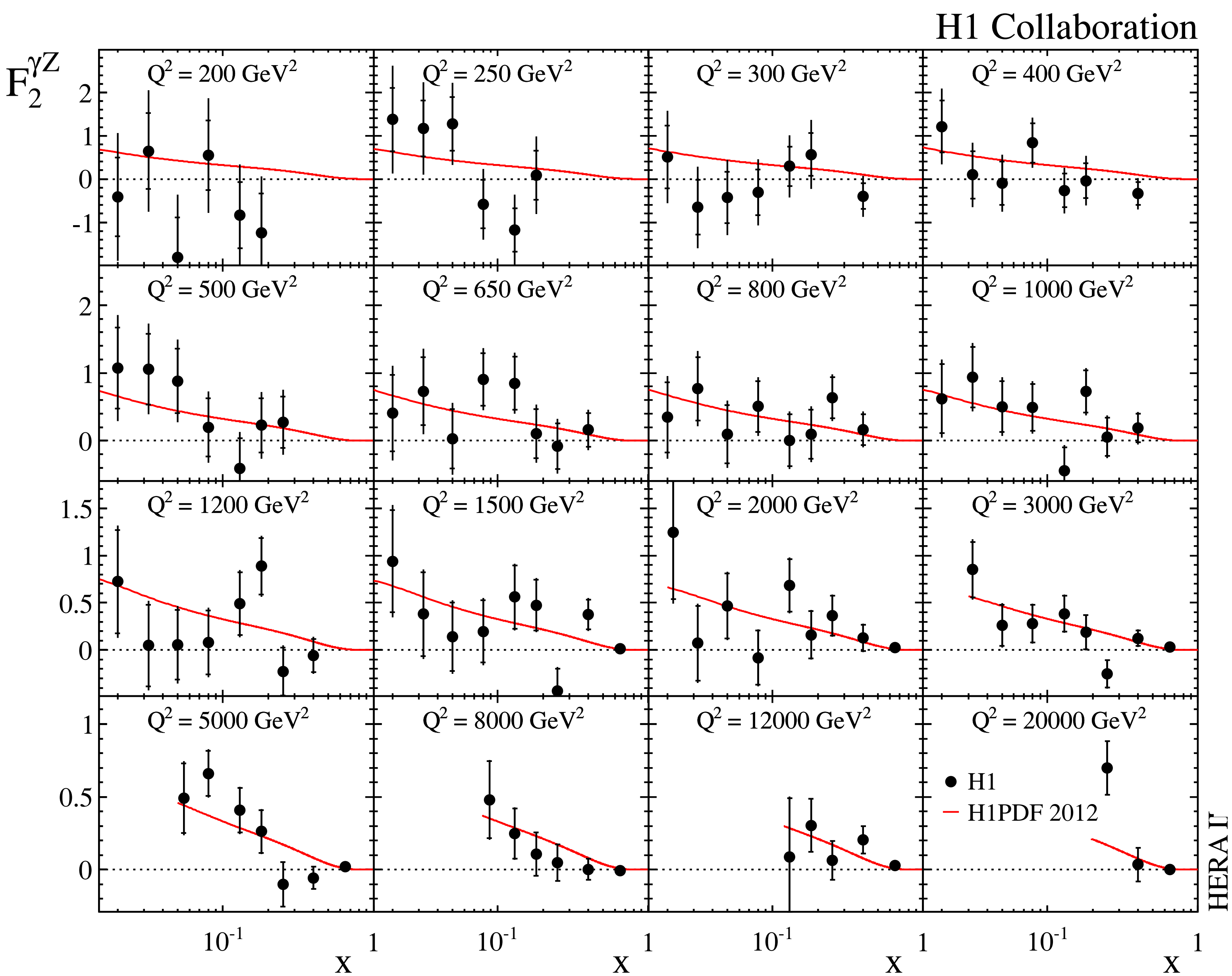

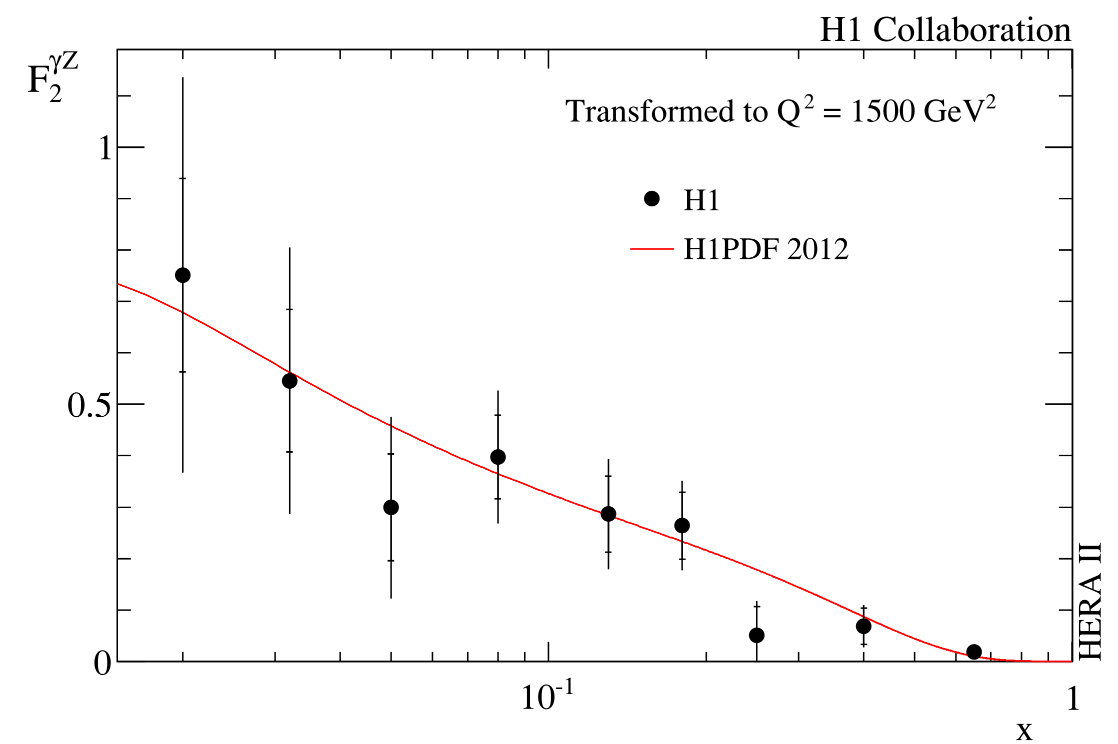

New H1 data are combined with all previously published H1 inclusive cross section measurements

854 data points averaged to 413 measurements
χ^2/ndf = 412/441 = 0.93

Normalisation shifts for H1 data after averaging

Source	Shift in units of standard deviation	Shift in % of cross section
$\delta^{\mathcal{L}1}$ (BH Theory)	-0.39	-0.19
$\delta^{\mathcal{L}2}$ (e^+ 94-97)	-0.46	-0.66
$\delta^{\mathcal{L}3}$ (e^- 98-99)	-0.69	-1.20
$\delta^{\mathcal{L}4}$ (e^+ 99-00)	-0.07	-0.10
$\delta^{\mathcal{L}5}$ (QEDC)	0.81	1.70
$\delta^{\mathcal{L}6}, \delta^{\mathcal{L}7}$ (e^+L+R)	0.84	0.80
$\delta^{\mathcal{L}8}, \delta^{\mathcal{L}9}$ (e^-L+R)	0.84	0.89

Precision medium Q^2 HERA-I data ~unshifted

New high Q^2 HERA-II data shifted by ~1.7% (less than 1 std.dev)

New PDF fit performed: can be thought of as a 'stepping-stone' towards HERAPDF2.0

$$
\begin{aligned}
xg(x) &= A_g x^{B_g}(1-x)^{C_g} - A'_g x^{B'_g}(1-x)^{25}\,, \\
xu_v(x) &= A_{u_v} x^{B_{u_v}}(1-x)^{C_{u_v}}\left(1+E_{u_v}x^2\right)\,, \\
xd_v(x) &= A_{d_v} x^{B_{d_v}}(1-x)^{C_{d_v}}\,, \\
x\overline{U}(x) &= A_{\overline{U}} x^{B_{\overline{U}}}(1-x)^{C_{\overline{U}}}\,, \\
x\overline{D}(x) &= A_{\overline{D}} x^{B_{\overline{D}}}(1-x)^{C_{\overline{D}}}\,.
\end{aligned}
$$

Parameter	Central Value	Lower Limit	Upper Limit
f_s	0.31	0.23	0.38
m_c (GeV)	1.4	1.35 (for $Q_0^2 = 1.8$ GeV)	1.65
m_b (GeV)	4.75	4.3	5.0
$Q^2_{\rm min}$ (GeV^2)	3.5	2.5	5.0
Q_0^2 (GeV^2)	1.9	1.5 ($f_s = 0.29$)	2.5 ($m_c = 1.6$, $f_s = 0.34$)

13 parameter fit: additional flexibility given to u_v and d_v compared to H1PDF2009 / HERAPDF1.0

Apply momentum/counting sum rules:

$$\int_0^1 dx \cdot (xu_v + xd_v + x\bar{U} + x\bar{D} + xg) = 1$$

$$\int_0^1 dx \cdot u_v = 2 \qquad \int_0^1 dx \cdot d_v = 1$$

Parameter constraints:
$B_{\rm Ubar} = B_{\rm Dbar}$
sea = 2 x (Ubar +Dbar)
Ubar = Dbar at x=0
f_s = sbar/Dbar

Q_0^2 = 1.9 GeV^2 (below m_c)
Q^2 > 3.5 GeV^2
2 x 10^{-4} < x < 0.65
Fits performed using RT-VFNS

Experimental uncertainties produced using RMS spread of 400 replica fits
Parameterisation uncertainty determined from envelope of 14 parameter fit & Q_0^2 variations
Error band is applied to central value fit ⇒ asymmetric errors since mean of replicas ≠ central fit

$$\chi^2 = \sum_i \frac{\left[\mu_i - m_i\left(1-\sum_j \gamma^i_j b_j\right)\right]^2}{\delta^2_{i,\rm unc} m_i^2 + \delta^2_{i,\rm stat}\mu_i m_i\left(1-\sum_j \gamma^i_j b_j\right)} + \sum_j b_j^2 + \sum_i \ln\frac{\delta^2_{i,\rm unc} m_i^2 + \delta^2_{i,\rm stat}\mu_i m_i}{\delta^2_{i,\rm unc}\mu_i^2 + \delta^2_{i,\rm stat}\mu_i^2}$$

modified χ^2 definition includes ln term to account for likelihood transition to χ^2 after error scaling

H1PDF 2012

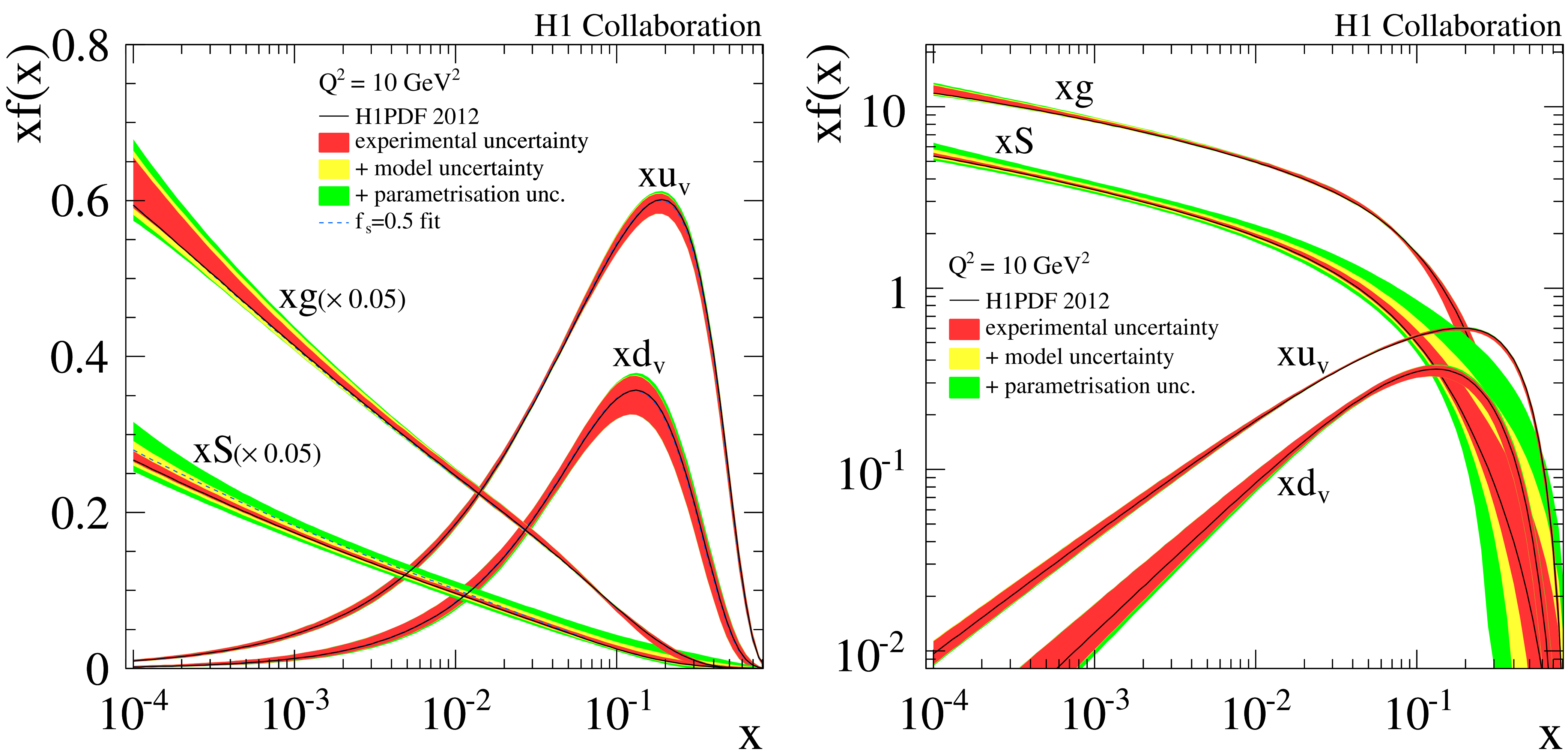

$\chi^2/\mathrm{ndf} = 1570/1461 = 1.07$

Fit with unsuppressed strange sea (f_s=0.5) is well within error bands

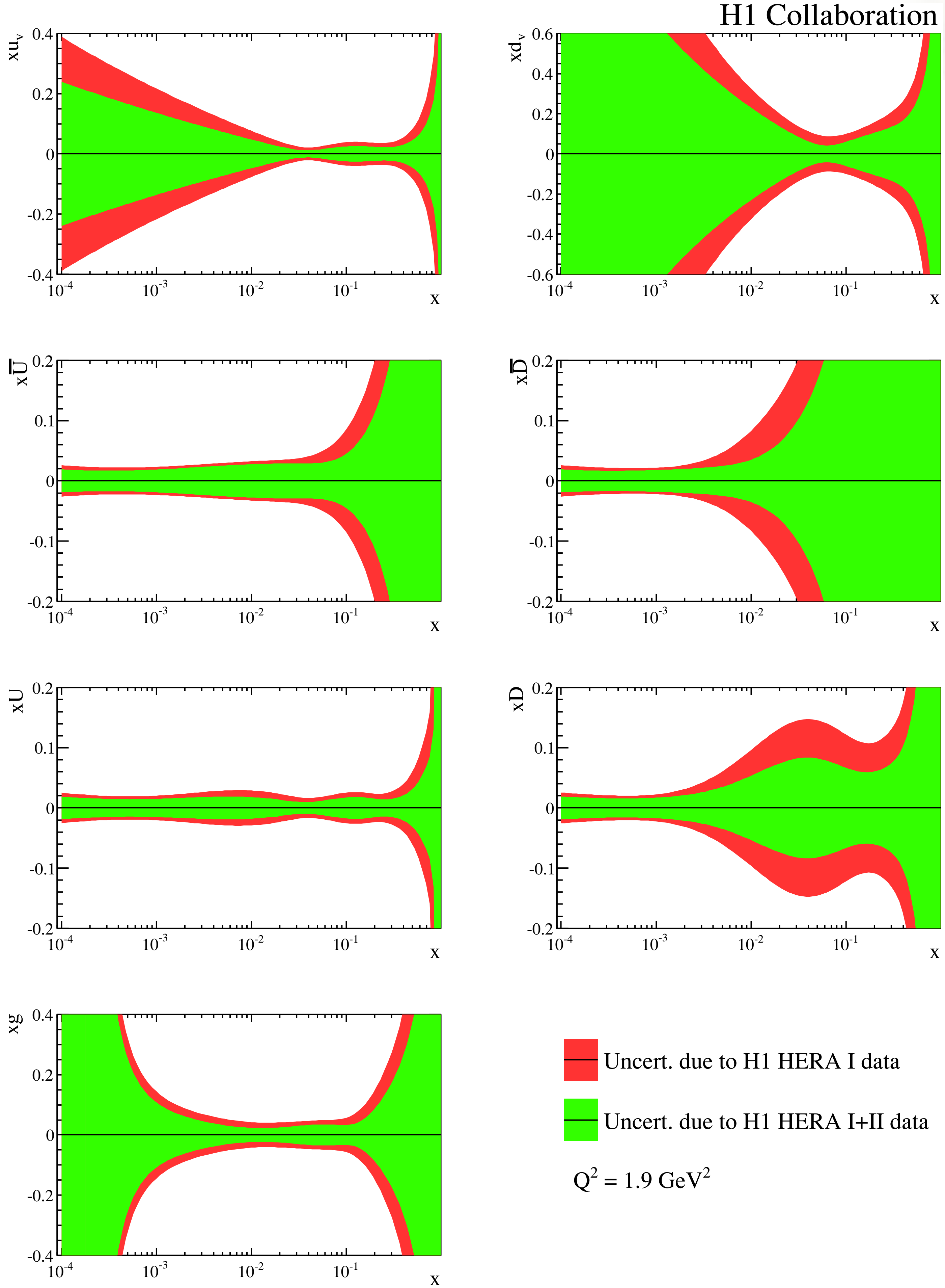

Comparison of PDF uncertainties from H1 fits with and without new HERA-II data

Large improvement in xd_v and xD over wide x range - driven by more precise CC e^+p data

Improvement in xu_v from NC at high x.
Error reduction at low x arises from sum rules

High x gluon is also improved from scaling violations

Compendium for HERAPDF

HERAPDF1.0
Combine NC and CC HERA-I data from H1 & ZEUS
Complete MSbar NLO fit
NLO: standard parameterisation with10 parameters
α_s = 0.1176 (fixed in fit)

HERAPDF1.5
Include additional NC and CC HERA-II data
Complete MSbar NLO and NNLO fit
NLO: standard parameterisation with 10 parameters

HERAPDF1.5f
NNLO: extended fit with 14 parameters

HERAPDF1.6
Include additional NC inclusive jet data $5 < Q^2 < 15000$
Complete MSbar NLO fit
NLO: standard parameterisation with 14 parameters
$\alpha_s = 0.1202 \pm 0.0013$ (exp) ± 0.004 (scales) free in fit

HERAPDF1.7
Include 41 additional F_2^{cc} data $4 < Q^2 < 1000$
Include 224 combined cross section points E_p=575/460 GeV
Complete MSbar NLO fit
NLO: standard parameterisation with 14 parameters

HERAPDF 2.0

HERAPDF2.0
Include final:
HERA-I low/medium Q^2 precision F_2
HERA-II high Q^2 polarised NC/CC data
HERA-II low/medium energy NC data
HERA-I+II F_2^{cc} combined data - almost ready
HERA-I+II multijet data - awaiting H1 publication

Combined F_2^{cc} now at 2nd stage of internal review

Expect journal submission ~ early Nov.

Final structure function measurements from H1 / ZEUS now published
Combination of the data is underway
New combination will include:
- HERA-I published data
- HERA-II published data
- low/medium energy E_p=575/460 GeV run data

Expect several fits:
- NLO vs NNLO
- NLO will be: inclusive NC/CC data & inclusive + F_2^{cc} (+ jets?)
- Include fit to α_S
- MC method for experimental errors will be used

Timescale ~ spring 2013 (DIS workshop?)

Conclusions

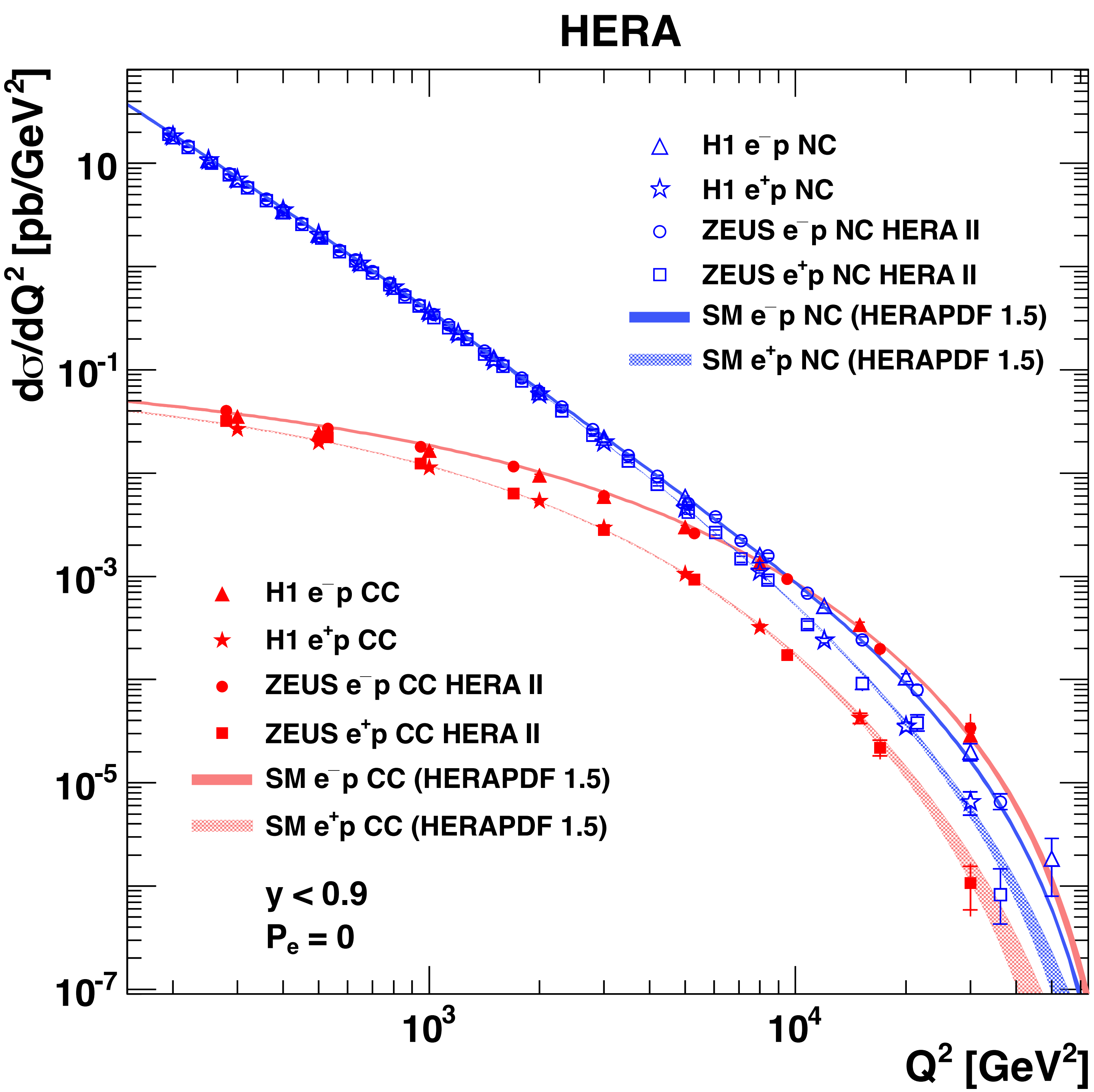

- H1 / ZEUS completed their final SF measurements
- New HERA-II data provide tighter constraints at high x / Q^2
- These data provide some of the most stringent constraints on PDFs
- Stress-test of QCD over 4 orders of mag. in Q^2
- DGLAP evolution works very well
- HERA data provide a self-consistent data set for complete flavour decomposition of the proton
- New combination of HERA data underway
- Combination ⇒ HERAPDF2.0 QCD fit

Backup Slides

H1 Systematic Error Source Correlation

Data set	$\delta^{\mathcal{L}}$		δ^{E}	δ^{θ}	δ^{h}	δ^{N}	δ^{B}	δ^{V}	δ^{S}	δ^{pol}
e^+ Combined low Q^2	$\delta^{\mathcal{L}1}$									
e^+ Combined low E_p	$\delta^{\mathcal{L}1}$									
e^+ NC 94-97	$\delta^{\mathcal{L}1}$	$\delta^{\mathcal{L}2}$	δ^{E1}	$\delta^{\theta 1}$	δ^{h1}	δ^{N1}	δ^{B1}	–	–	–
e^+ CC 94-97	$\delta^{\mathcal{L}1}$	$\delta^{\mathcal{L}2}$	–	–	δ^{h1}	δ^{N1}	δ^{B1}	δ^{V1}	–	–
e^- NC 98-99	$\delta^{\mathcal{L}1}$	$\delta^{\mathcal{L}3}$	δ^{E1}	$\delta^{\theta 2}$	δ^{h1}	δ^{N1}	δ^{B1}	–	–	–
e^- NC 98-99 *high* y	$\delta^{\mathcal{L}1}$	$\delta^{\mathcal{L}3}$	δ^{E1}	$\delta^{\theta 2}$	δ^{h1}	δ^{N1}	–	–	δ^{S1}	–
e^- CC 98-99	$\delta^{\mathcal{L}1}$	$\delta^{\mathcal{L}3}$	–	–	δ^{h1}	δ^{N1}	δ^{B1}	δ^{V2}	–	–
e^+ NC 99-00	$\delta^{\mathcal{L}1}$	$\delta^{\mathcal{L}4}$	δ^{E1}	$\delta^{\theta 2}$	δ^{h1}	δ^{N1}	δ^{B1}	–	δ^{S1}	–
e^+ CC 99-00	$\delta^{\mathcal{L}1}$	$\delta^{\mathcal{L}4}$	–	–	δ^{h1}	δ^{N1}	δ^{B1}	δ^{V2}	–	–
e^+ NC *high* y	$\delta^{\mathcal{L}5}$	$\delta^{\mathcal{L}6}, \delta^{\mathcal{L}7}$	δ^{E2}	$\delta^{\theta 3}$	δ^{h2}	δ^{N2}	–	–	δ^{S2}	–
e^- NC *high* y	$\delta^{\mathcal{L}5}$	$\delta^{\mathcal{L}8}, \delta^{\mathcal{L}9}$	δ^{E2}	$\delta^{\theta 3}$	δ^{h2}	δ^{N2}	–	–	δ^{S2}	–
e^+ NC L	$\delta^{\mathcal{L}5}$	$\delta^{\mathcal{L}6}$	δ^{E2}	$\delta^{\theta 3}$	δ^{h2}	δ^{N2}	δ^{B1}	–	–	δ^{P1}
e^+ CC L	$\delta^{\mathcal{L}5}$	$\delta^{\mathcal{L}6}$	–	–	δ^{h2}	δ^{N3}	δ^{B1}	δ^{V3}	–	δ^{P1}
e^+ NC R	$\delta^{\mathcal{L}5}$	$\delta^{\mathcal{L}7}$	δ^{E2}	$\delta^{\theta 3}$	δ^{h2}	δ^{N2}	δ^{B1}	–	–	δ^{P2}
e^+ CC R	$\delta^{\mathcal{L}5}$	$\delta^{\mathcal{L}7}$	–	–	δ^{h2}	δ^{N3}	δ^{B1}	δ^{V3}	–	δ^{P2}
e^- NC L	$\delta^{\mathcal{L}5}$	$\delta^{\mathcal{L}8}$	δ^{E2}	$\delta^{\theta 3}$	δ^{h2}	δ^{N2}	δ^{B1}	–	–	δ^{P3}
e^- CC L	$\delta^{\mathcal{L}5}$	$\delta^{\mathcal{L}8}$	–	–	δ^{h2}	δ^{N3}	δ^{B1}	δ^{V3}	–	δ^{P3}
e^- NC R	$\delta^{\mathcal{L}5}$	$\delta^{\mathcal{L}9}$	δ^{E2}	$\delta^{\theta 3}$	δ^{h2}	δ^{N2}	δ^{B1}	–	–	δ^{P4}
e^- CC R	$\delta^{\mathcal{L}5}$	$\delta^{\mathcal{L}9}$	–	–	δ^{h2}	δ^{N3}	δ^{B1}	δ^{V3}	–	δ^{P4}

correlation of H1 systematic error sources

$\delta^{\mathcal{L}1}$ → 0.5% BH theoretical error HERA-I

$\delta^{\mathcal{L}5}$ → 2.3% Compton lumi error HERA-II

$\delta^{\mathcal{L}6\text{-}9}$ → 1.5% Compton unc. error HERA-II

Data Period	Global Normalisation	Per Period Normalisation	Total Normalisation
e^+ Combined low Q^2	0.993	–	0.993
e^+ Combined low E_p	0.993	–	0.993
HERA I e^+ 94-97	0.993	0.999	0.992
HERA I e^- 98-99	0.993	1.003	0.996
HERA I e^+ 99-00	0.993	1.005	0.998
HERA II e^+ L	1.029	0.991	1.020
HERA II e^+ R	1.029	1.013	1.042
HERA II e^- L	1.029	1.010	1.039
HERA II e^- R	1.029	1.014	1.043

normalisations from H1PDF 2012

Low Q^2 data shifted by -0.7%
HERA-I high Q^2 by -0.3%
HERA-II high Q^2 by +2 to +4%

All shifts are <1.3 std.devs

HERAPDF

HERAPDF1.0
Combine NC and CC HERA-I data from H1 & ZEUS
Complete MSbar NLO fit
NLO: standard parameterisation with10 parameters
$\alpha_s = 0.1176$ (fixed in fit)

desy-09-158

HERAPDF1.5
Include additional NC and CC HERA-II data
Complete MSbar NLO and NNLO fit
NLO: standard parameterisation with10 parameters
HERAPDF1.5f
NNLO: extended fit with 14 parameters

H1-10-142 / ZEUS-prel-10-018

$$xf(x,Q_0^2) = A \cdot x^B \cdot (1-x)^C \cdot (1 + Dx + Ex^2)$$

xg, xu_v, xd_v, $x\bar{U}$, $x\bar{D}$ → xg, $xU = xu + xc$, $xD = xd + xs$, $x\bar{U} = x\bar{u} + x\bar{c}$, $x\bar{D} = x\bar{d} + x\bar{s}$ →

$$\begin{aligned} xg(x) &= A_g x^{B_g}(1-x)^{C_g}, \\ xu_v(x) &= A_{u_v} x^{B_{u_v}}(1-x)^{C_{u_v}}\left(1 + E_{u_v}x^2\right), \\ xd_v(x) &= A_{d_v} x^{B_{d_v}}(1-x)^{C_{d_v}}, \\ x\bar{U}(x) &= A_{\bar{U}} x^{B_{\bar{U}}}(1-x)^{C_{\bar{U}}}, \\ x\bar{D}(x) &= A_{\bar{D}} x^{B_{\bar{D}}}(1-x)^{C_{\bar{D}}}. \end{aligned}$$

$x\bar{s} = f_s x\bar{D}$ strange sea is a fixed fraction f_s of $\bar{D}$ at Q_0^2

Apply momentum/counting sum rules:

$$\int_0^1 dx \cdot (xu_v + xd_v + x\bar{U} + x\bar{D} + xg) = 1$$

$$\int_0^1 dx \cdot u_v = 2 \qquad \int_0^1 dx \cdot d_v = 1$$

Parameter constraints:
$B_{uv} = B_{dv}$
$B_{Ubar} = B_{Dbar}$
sea = 2 x (Ubar +Dbar)
Ubar = Dbar at x=0

Q_0^2 = 1.9 GeV^2 (below m_c)
Q^2 > 3.5 GeV^2
$2 \times 10^{-4} < x < 0.65$
Fits performed using RT-VFNS

HERAPDF1.0 central values:

	A	B	C	E
xg	6.8	0.22	9.0	
xu_v	3.7	0.67	4.7	9.7
xd_v	2.2	0.67	4.3	
$x\bar{U}$	0.113	–0.165	2.6	
$x\bar{D}$	0.163	–0.165	2.4	

χ^2/ndf = 574/582

Experimental systematic sources of uncertainty allowed to float in fit
Include model assumptions into uncertainty:
f_s , m_c , m_b , $Q^2{}_0$, $Q^2{}_{min}$

Variation	Standard Value	Lower Limit	Upper Limit
f_s	0.31	0.23	0.38
m_c [GeV]	1.4	$1.35^{(a)}$	1.65
m_b [GeV]	4.75	4.3	5.0
Q^2_{min} [GeV^2]	3.5	2.5	5.0
Q^2_0 [GeV^2]	1.9	$1.5^{(b)}$	$2.5^{(c,d)}$

$^{(a)}Q^2_0 = 1.8$ $^{(c)}m_c = 1.6$
$^{(b)}f_s = 0.29$ $^{(d)}f_s = 0.34$

Excellent consistency of input data allow standard statistical error definition:
$\Delta\chi^2 = 1$

Exclusive jet data required for free α_s fit
See talk of Krzysztof Nowak

In 14 parameter fit:
release $B_{uv} = B_{dv}$ constraint
allow more flexible gluon

$$xg(x,Q_0^2) = A \cdot x^B \cdot (1-x)^C - A' \cdot x^{B'} \cdot (1-x)^{25}$$

allows for valence-like or negative gluon at Q_0^2

Charm Content of the Proton

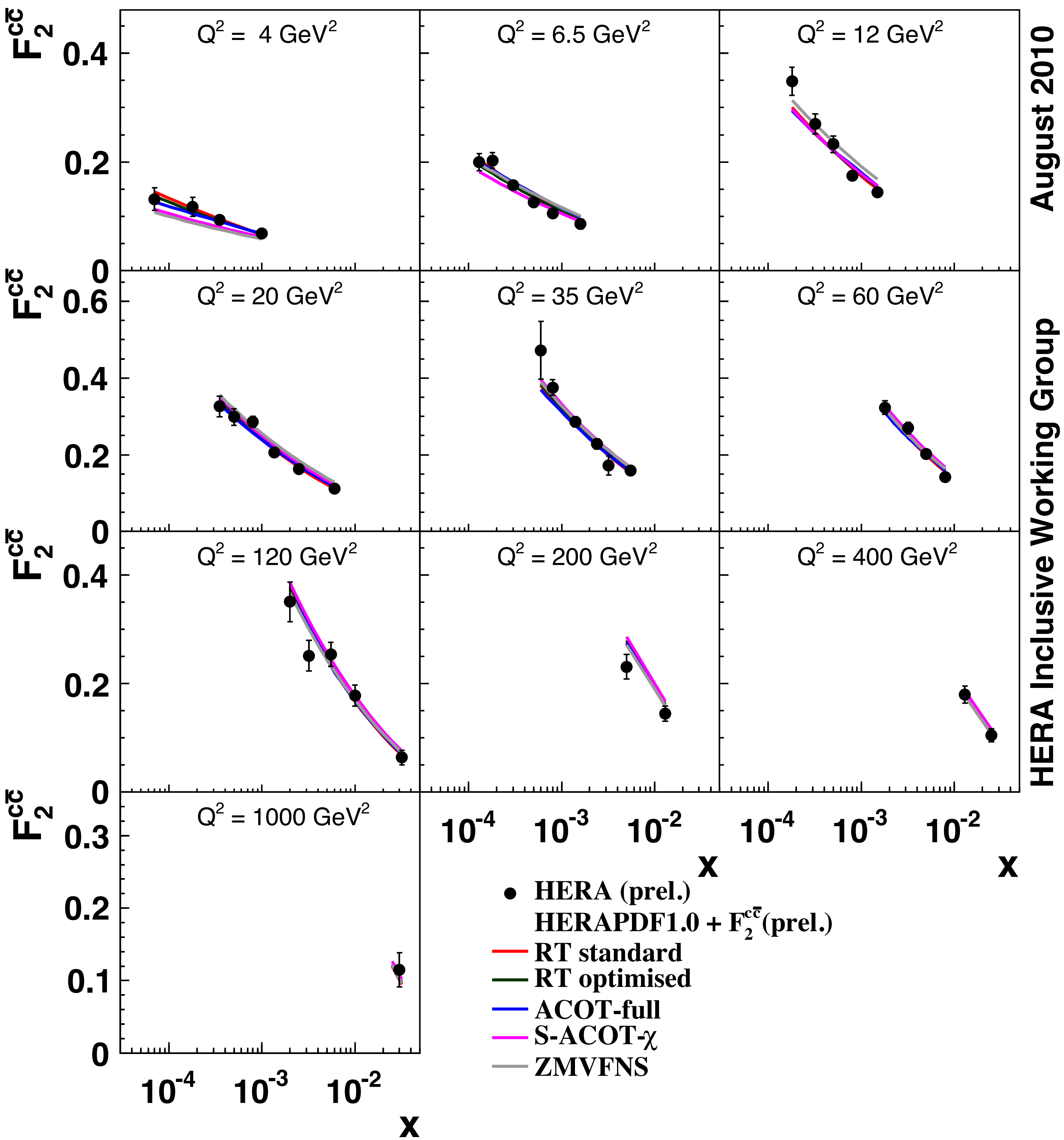

The inclusive charm content of proton can be measured in several methods: D* decays , impact parameter significance... Combination yields ~5-10% precision

Data cover wide phase space region including charm threshold region

Theory predictions have small spread
⇒ use optimised m_c parameter

Spread of LHC Z/W production predictions is reduced ~4.5% → ~0.7%
when using optimal value of m_c

DIS Jet Cross Sections

ZEUS inclusive jets	39 pb^{-1}	$Q^2 > 125$	Nucl. Phys. B765 (2007) 1-30
ZEUS inclusive jets	82 pb^{-1}	$Q^2 > 125$	Phys. Lett. B649 (2007) 12
H1 inclusive jets	395 pb^{-1}	$150 < Q^2 < 15000$	EPJ C65 (2010) 363-383
H1 inclusive jets	44 pb^{-1}	$5 < Q^2 < 100$	EPJ C67 (2010) 1-24

Jet data bring significant sensitivity to α_S
Disentangles correlation between $xg(x,Q^2)$ and α_S

HERAPDF1.6 : Simultaneous NLO QCD fit to
- combined NC inclusive cross section data
- combined CC inclusive cross sections data
- normalised H1/ZEUS inclusive jet data

$$\alpha_S(M_Z) = 0.1202 \pm 0.0013\ (\mathrm{exp}) \pm 0.0007\ (\mathrm{model}) \pm 0.0012\ (\mathrm{hadronisation})\ ^{+0.0045}_{-0.0036}\ (\mathrm{scales})$$

Only combined PDF / α_S fit on the market

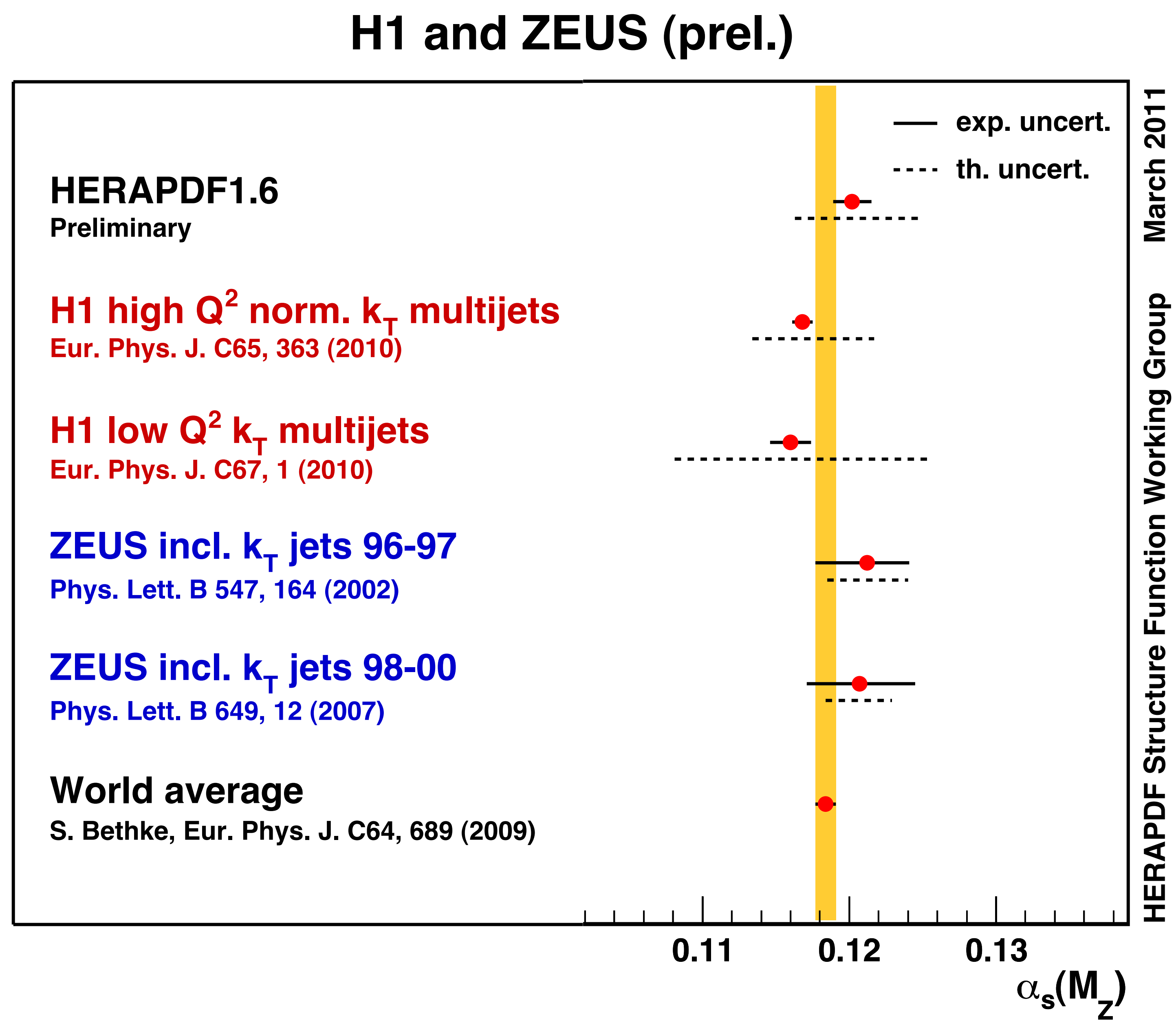

High Q^2 NC Multi-jets

H1prelim-11-032

New H1 measurement of inclusive, dijet and trijet rates

<u>First measurement</u> of double diff'l trijet cross section

Significantly reduced systematic errors

1% hadronic scale uncertainty

For now - unnormalised cross sections...

Jets in Breit frame: $5 < P_T < 50$ GeV
$M_{12} > 16$ GeV

Greater sensitivity to α_s with more jets

High Q^2 and large jet $P_T \Rightarrow$ multi-scale QCD problem

Good description in NLO

(worse for di-jets at low $\langle P_T \rangle$ ...)

NLO calculation $\mu_R = \mu_F = \sqrt{\frac{1}{2}(Q^2 + P_T^2)}$

scales varied by factors of 2 for uncertainty

Trijet Cross Section

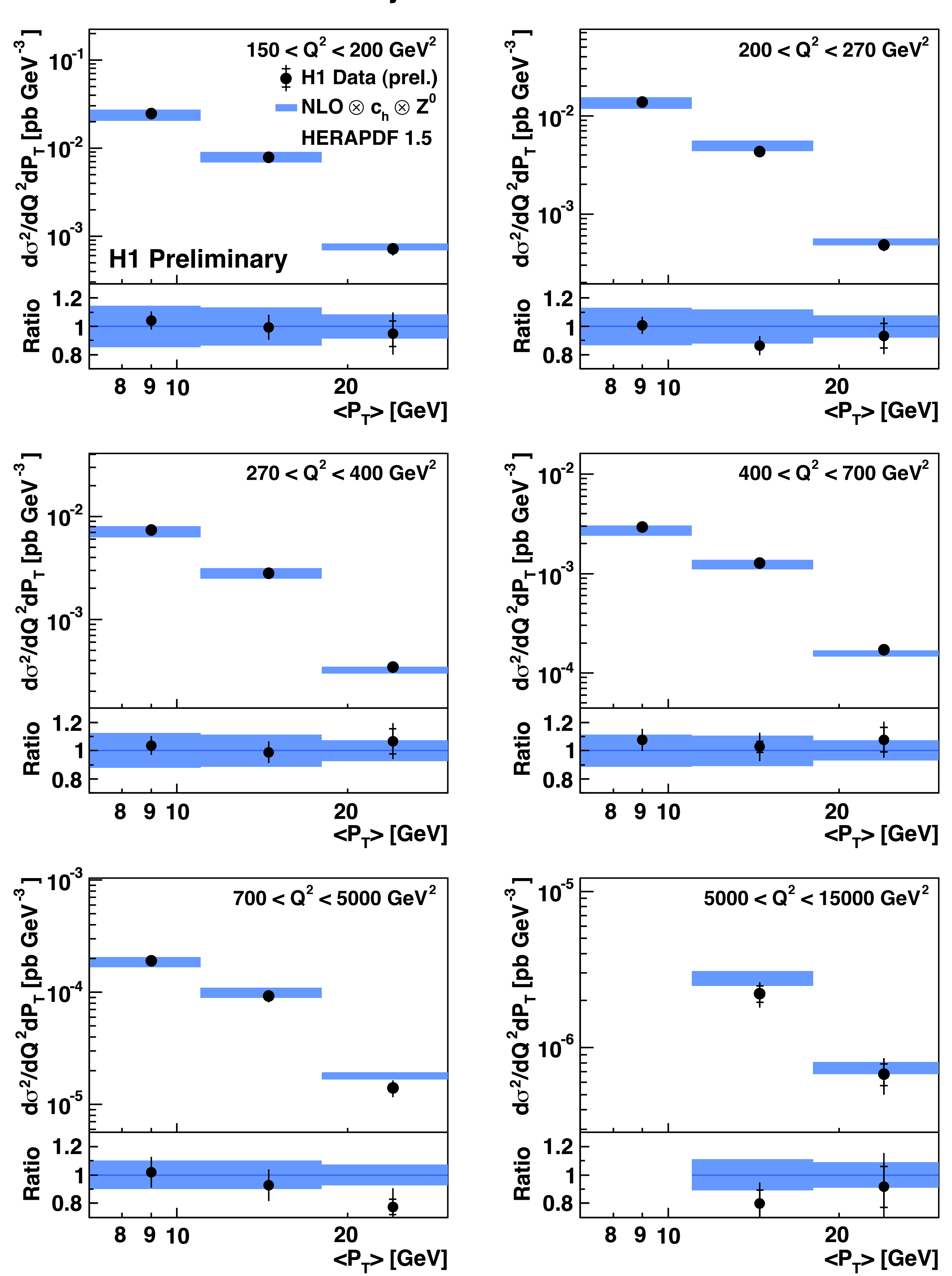

High Q^2 NC Multi-jets

H1prelim-11-032

Di-jet rates in reasonable agreement
~10% discrepancy at low $\langle P_T \rangle$
Data want smaller α_s or smaller xg ?

Extract α_s independently for each jet data set in NLO
PDF uncertainty from CT10 error propagation

Inclusive jets:

$$\alpha_s(M_Z) = 0.1190 \pm 0.0021(exp.) \pm 0.0020(pdf)^{+0.0050}_{-0.0056}(th.)$$

Dijets:

$$\alpha_s(M_Z) = 0.1146 \pm 0.0022(exp.) \pm 0.0021(pdf)^{+0.0044}_{-0.0045}(th.)$$

Trijets:

$$\alpha_s(M_Z) = 0.1196 \pm 0.0016(exp.) \pm 0.0010(pdf)^{+0.0055}_{-0.0039}(th.)$$

Achieved ~1% experimental precision on α_s
Theoretical uncertainty (scales) dominate ~4%
PDF uncertainty ~1%

To come:
Use of normalised cross sections
cancellation of systematic uncertainties
→ reduced error for α_s